NAVAL POSTGRADUATE SCHOOL
MONTEREY, CALIFORNIA

THESIS

STEP FREQUENCY WAVEFORM DESIGN AND ANALYSIS USING THE AMBIGUITY FUNCTION

by

Paulo A. Soares

June, 1996

Thesis Advisor: Gurnam S. Gill

Approved for public release; distribution is unlimited.

REPORT DOCUMENTATION PAGE

Form Approved OMB No. 0704-0188

1. AGENCY USE ONLY *(Leave blank)*	2. REPORT DATE June 1996	3. REPORT TYPE AND DATES COVERED Master's Thesis	
4. TITLE AND SUBTITLE STEP FREQUENCY WAVEFORM DESIGN AND ANALYSIS USING THE AMBIGUITY FUNCTION		5. FUNDING NUMBERS	
6. AUTHOR(S) Soares, Paulo A.			
7. PERFORMING ORGANIZATION NAME(S) AND ADDRESS(ES) Naval Postgraduate School Monterey CA 93943-5000		8. PERFORMING ORGANIZATION REPORT NUMBER	
9. SPONSORING/MONITORING AGENCY NAME(S) AND ADDRESS(ES)		10. SPONSORING/MONITORING AGENCY REPORT NUMBER	
11. SUPPLEMENTARY NOTES The views expressed in this thesis are those of the author and do not reflect the official policy or position of the Department of Defense or the U.S. Government.			
12a. DISTRIBUTION/AVAILABILITY STATEMENT Approved for public release; distribution is unlimited.		12b. DISTRIBUTION CODE	

13. ABSTRACT *(maximum 200 words)*

This thesis investigates the use of the step frequency waveform, its design and analysis using the ambiguity function. The step frequency waveform consists of a series of N pulses each with a pulse width of τ, and whose frequency is increased from pulse to pulse in steps of Δf. A design procedure for detection of small targets with a surface (land or sea) based step frequency radar employing a high pulse repetition frequency (PRF) waveform is developed. The proposed method determines the waveform parameters for given radar specifications. A simple graphical implementation as well as a computer implementation are presented. The theoretical dimensions of the step frequency waveform are defined and verified for some waveforms with parameters similar to the waveform of interest. Finally, the ambiguity function is used to analyze the step frequency waveform.

14. SUBJECT TERMS Step Frequency Radar, Step Frequency Waveform, High Range Resolution, Ambiguity Function, Ambiguity Diagram		15. NUMBER OF PAGES 104
		16. PRICE CODE

17. SECURITY CLASSIFICATION OF REPORT Unclassified	18. SECURITY CLASSIFICATION OF THIS PAGE Unclassified	19. SECURITY CLASSIFICATION OF ABSTRACT Unclassified	20. LIMITATION OF ABSTRACT UL

STEP FREQUENCY WAVEFORM DESIGN
AND ANALYSIS USING THE AMBIGUITY FUNCTION

Paulo A. Soares
Lieutenant, Portuguese Navy
B.S., Portuguese Naval Academy, 1989

Submitted in partial fulfillment
of the requirements for the degree of

MASTER OF SCIENCE IN APPLIED PHYSICS

from the

NAVAL POSTGRADUATE SCHOOL
June 1996

ABSTRACT

This thesis investigates the use of the step frequency waveform, its design and analysis using the ambiguity function. The step frequency waveform consists of a series of N pulses each with a pulse width of τ, and whose frequency is increased from pulse to pulse in steps of Δf. A design procedure for detection of small targets with a surface (land or sea) based step frequency radar employing a high pulse repetition frequency (PRF) waveform is developed. The proposed method determines the waveform parameters for given radar specifications. A simple graphical implementation as well as a computer implementation are presented. The theoretical dimensions of the step frequency waveform are defined and verified for some waveforms with parameters similar to the waveform of interest. Finally, the ambiguity function is used to analyze the step frequency waveform.

TABLE OF CONTENTS

LIST OF FIGURES

I. INTRODUCTION

A. BACKGROUND

Over the past few years the applications for imaging or multidimensional high resolution radar systems have expanded greatly. This has been primarily due to the improvements in both the waveform generation and the signal processing needed to support the radar imaging technology. Higher resolution measurements give more information about the target, but also require more detailed measurements of the target, thus translating into increased radar system requirements and complexity. The theory of high resolution radar has been around for some time, but extensive applications of the technology have appeared only recently due to new developments in technology. Recent applications of high resolution techniques have appeared in a variety of areas, including:

- Modeling and analysis or radar targets;

- Diagnostic methods for target radar cross section reduction;

- Development of target detection, discrimination, recognition, and classification techniques;

- Improved radar detectability performance;

- Diagnostic methods to support the medical and physical sciences.

High range resolution (HRR) in radar has many good uses. Among these a few are listed below:

- Enhancement of target-to-clutter ratio;

- Accurate range measurement;

- Resolution of multiple targets - raid count;

- Target range profile and size;

- Target classification;

- Recognition and avoidance of deception ECM;

- Measurement of range rate without doppler.

HRR is achieved by using a large bandwidth. In ultrawideband (UWB) waveforms, large bandwidth is obtained by decreasing the pulse width. However, when the pulse width is too narrow, sampling becomes problematic and is limited by existing analog-to-digital (A/D) technology. In conventional pulse compression (PC), a large bandwidth is obtained by modulation inside the pulse. In both approaches, the instantaneous bandwidth is large which requires a high A/D sampling rate. In the step frequency waveform, the bandwidth is increased sequentially (instead of instantaneously as in the previous cases) over many pulses within a burst by stepping the frequency of each pulse. By keeping the instantaneous bandwidth low, the requirements for A/D sampling rates are lowered considerably. The A/D sampling rate is a bottleneck in HRR radar design. Thus , the step frequency seems to be a good waveform for HRR.

A step frequency radar operates by transmitting a waveform composed of a number of increasing stepped frequencies. A coherent I-Q detector measures both the in-phase and in-quadrature components of the received signal at each of the frequency steps. The phase information included in this complex sequence allows for accurate distance measurements.

B. OVERVIEW

This thesis discusses the step frequency waveform design and its analysis using the ambiguity function. In Chapter II the fundamental principles of the step frequency radar are explained. The step frequency waveform is defined and the waveform processing is explained. Also in this chapter the implementation of the radar system is described. In Chapter III the waveform design method is developed. Both graphical and computer implementations are shown and used to compute the waveform parameters. The ambiguity function is introduced in Chapter IV. Some important examples of the ambiguity function are shown. The theoretical dimensions of the ambiguity diagram are defined and then verified with a few cases of interest. These theoretical dimensions are then used to define the ambiguity diagram of a waveform with a large number of pulses, which for this reason is difficult to compute and plot with the desired resolution. Finally, in Chapter V the conclusions of this thesis are presented. The MATLAB codes used are given in Appendix B.

II. STEP FREQUENCY RADAR - OPERATING PRINCIPLE

A. STEP FREQUENCY WAVEFORM

The step frequency waveform consists of a series of N pulses each with a pulse width of τ, and whose frequency is increased from pulse to pulse in steps of Δf, as shown in Figure 1. The frequency of the nth transmitted pulse is given by

$$f_n = f_0 + (n-1)\Delta f, \tag{2.1}$$

where

$$f_0 = \text{nominal carrier frequency;}$$

$$\Delta f = \text{frequency step size;}$$

$$n = 1, 2, 3, ..., N.$$
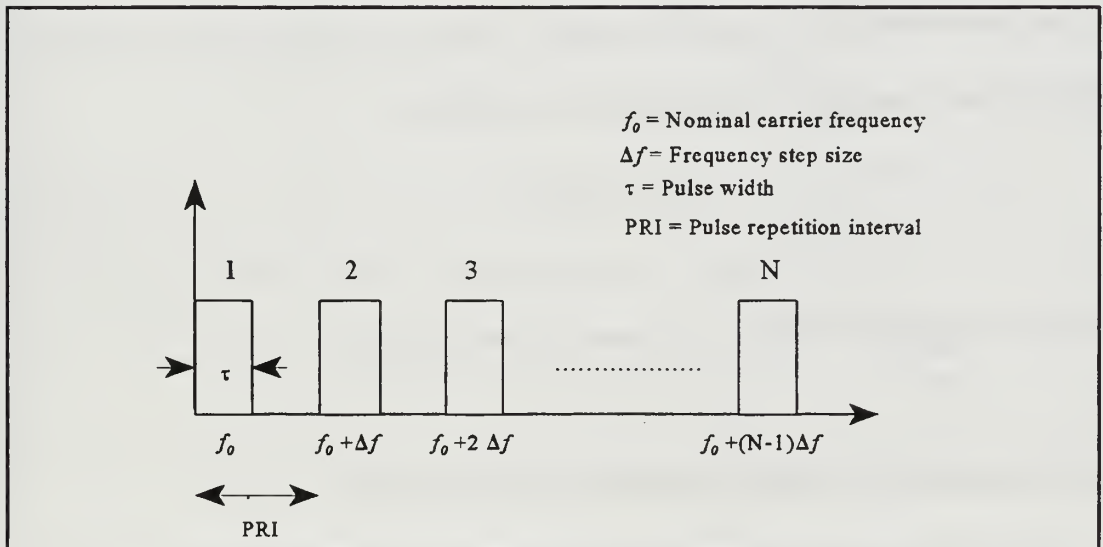
Figure 1.   Step Frequency Waveform.

The total effective bandwidth of the step frequency waveform is given by

$$B_{eff} = N\Delta f. \tag{2.2}$$

The range resolution for this waveform is not the conventional value of $c\tau/2$. The synthetic range resolution obtained by coherently processing a series of N returns from the target is given by

$$\Delta R = \frac{c}{2B_{eff}} = \frac{c}{2N\Delta f}, \tag{2.3}$$

where ΔR is the processed range resolution in meters and c is the speed of light (3×10^8m/sec). As can be seen from Equation 2.3, the range resolution can be improved by either increasing the number of pulses or the frequency step size.

The coherent processing interval (CPI) is the total time duration in which returns from a target are collected for signal processing. Thus the CPI is just the product of the number of pulses N, and the pulse repetition interval (PRI);

$$CPI = N(PRI). \tag{2.4}$$

The coherent processing interval is also known as the burst time.

B.   SYSTEM DESCRIPTION AND IMPLEMENTATION

The implementation of the step frequency radar is similar to the coherent Pulse-Doppler radar. The system implementation can be observed in Figure 2. The core of the system is a coherent step frequency synthesizer with an output frequency called f_{syn}, which

$$f_x = f_{STALO} + f_{STN} + f_{COHO}$$

STALO

Up-converter
Mixer

f_{STALO}

Pulse
Modulator

Amplifier

Circulator

Antenna

Receiver
Protection

$f_{STN} + f_{COHO}$

Stepped
Frequency
Synthesizer

f_{STN}

Mixer

$f_{STN} + f_{COHO}$

COHO

f_{COHO}

f_{COHO}

Coherent
Detector

I

Q
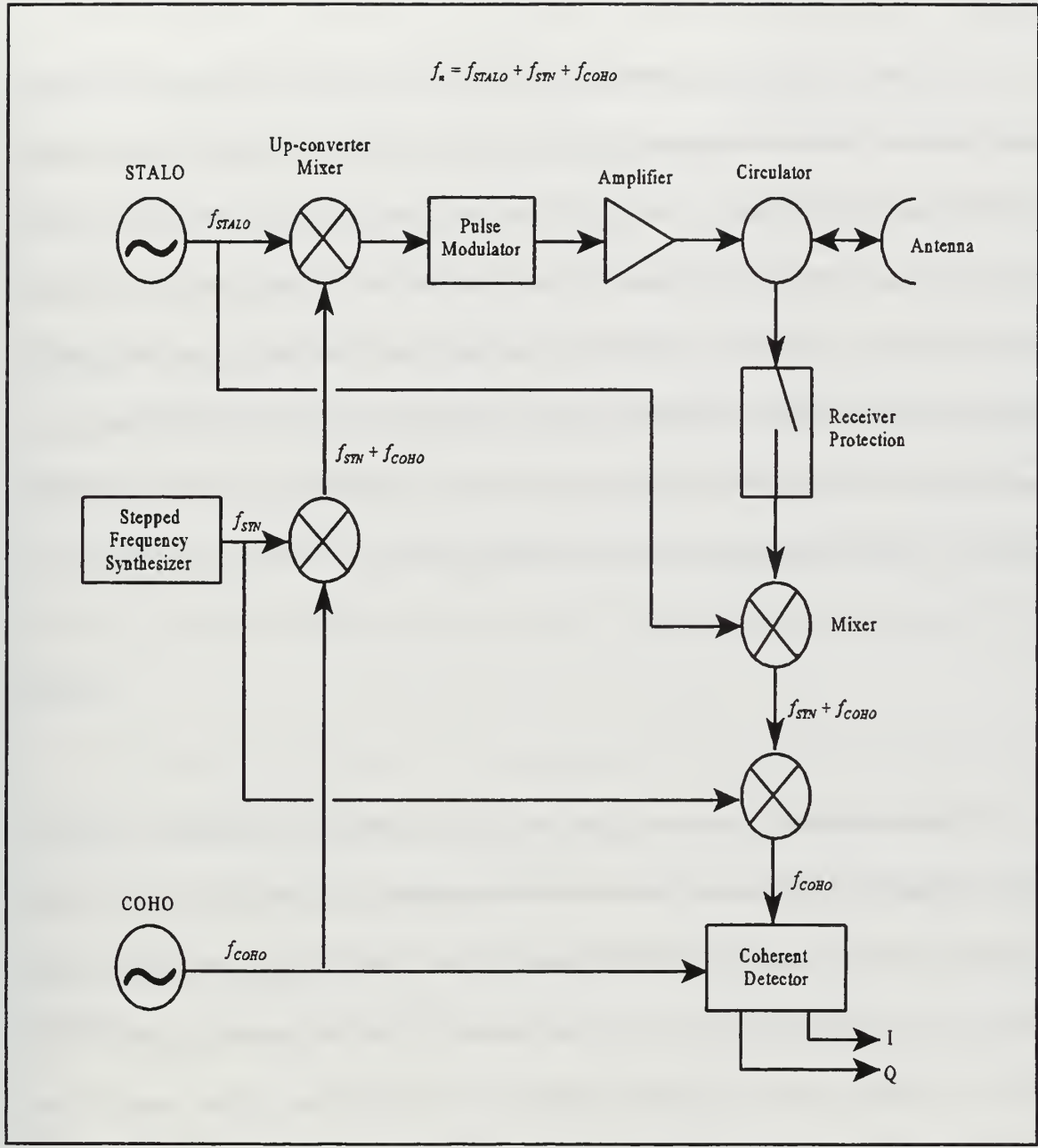
Figure 2.   Block Diagram of a Step Frequency Radar.

7

is stepped from pulse to pulse by a fixed step size, Δf. Therefore, we can write

$$f_{syn} = (n-1)\Delta f. \qquad (2.5)$$

The frequency of a local coherent oscillator (COHO), f_{coho}, is first mixed with the output frequency of the step frequency synthesizer, f_{syn} . Then the sum frequency is converted to the final transmitted frequency by mixing it with the frequency of the stable local oscillator (STALO), f_{stalo} . The sum frequency of this second mixer is then pulse modulated and amplified before the transmission occurs. Each transmitted pulse will have a carrier frequency comprised of three different components: the fixed IF frequency, f_{coho}, the fixed RF frequency, f_{stalo}, and the variable frequency of the stepped frequency synthesizer, f_{syn} . Thus, the carrier frequency of the nth pulse is given by the following equation:

$$f_n = f_{stalo} + f_{coho} + f_{syn} = f_0 + (n-1)\Delta f. \qquad (2.6)$$

In the receiver side, the return signal is first down converted by mixing it with f_{stalo} . The resulting signal is further down converted to intermediate frequency (IF) by mixing with f_{syn} . The output signal obtained after the second mixer is the IF signal. The signal is then divided into two different channels, the in-phase channel (I), and the quadrature channel (Q). Both, the in-phase and the quadrature signals are mixed with the output signal of the coherent oscillator. The first is mixed directly and the second is mixed with the COHO signal after this last one has been shifted 90 degrees. The I and Q components, both in the video frequency range, are sampled by an A/D converter at a rate equal to the inverse of the pulse width.

Each complex sample is usually called *range bin*, thus range bin may be defined as a memory location for temporary storage of successive pairs of numbers representing the I and Q samples of the radar return received at a given point in the interpulse period. A separate bin therefore must be provided for each sampling interval (range gate). To the extent that range is unambiguous, the numbers stored in any one bin represent successive returns from a single range increment, hence the name range bin. Because of the correspondence of the range bins to the sampling intervals (when A/D conversion follows I and Q detection), range bin has come to be used synonymously with *sampling interval* as well as *range gate*.

Sampled returns from incoming pulses are stored im memory until all the pulses within the same burst have been received and can be processed. Figure 3 describes the organization of sample storage in memory. Complex samples for each range bin are transformed by taking the FFT of samples in each range bin, resulting in a high resolution range profile (HRR profile).

One important advantage of the step frequency radar compared with other radars which also use wideband waveforms, is that in the former the narrow instantaneous bandwidth does not require a high analog to digital sampling rate which can be a major limitation in the system design. On the other hand, the step frequency radar may require more complex signal processing.

N samples

1
f_0

2
$f_0 + \Delta f$

3
$f_0 + 2\Delta f$

4
$f_0 + 3\Delta f$

5
$f_0 + 4\Delta f$

6
$f_0 + 5\Delta f$

N
$f_0 + (N-1)\Delta f$

Range cells

Range bin
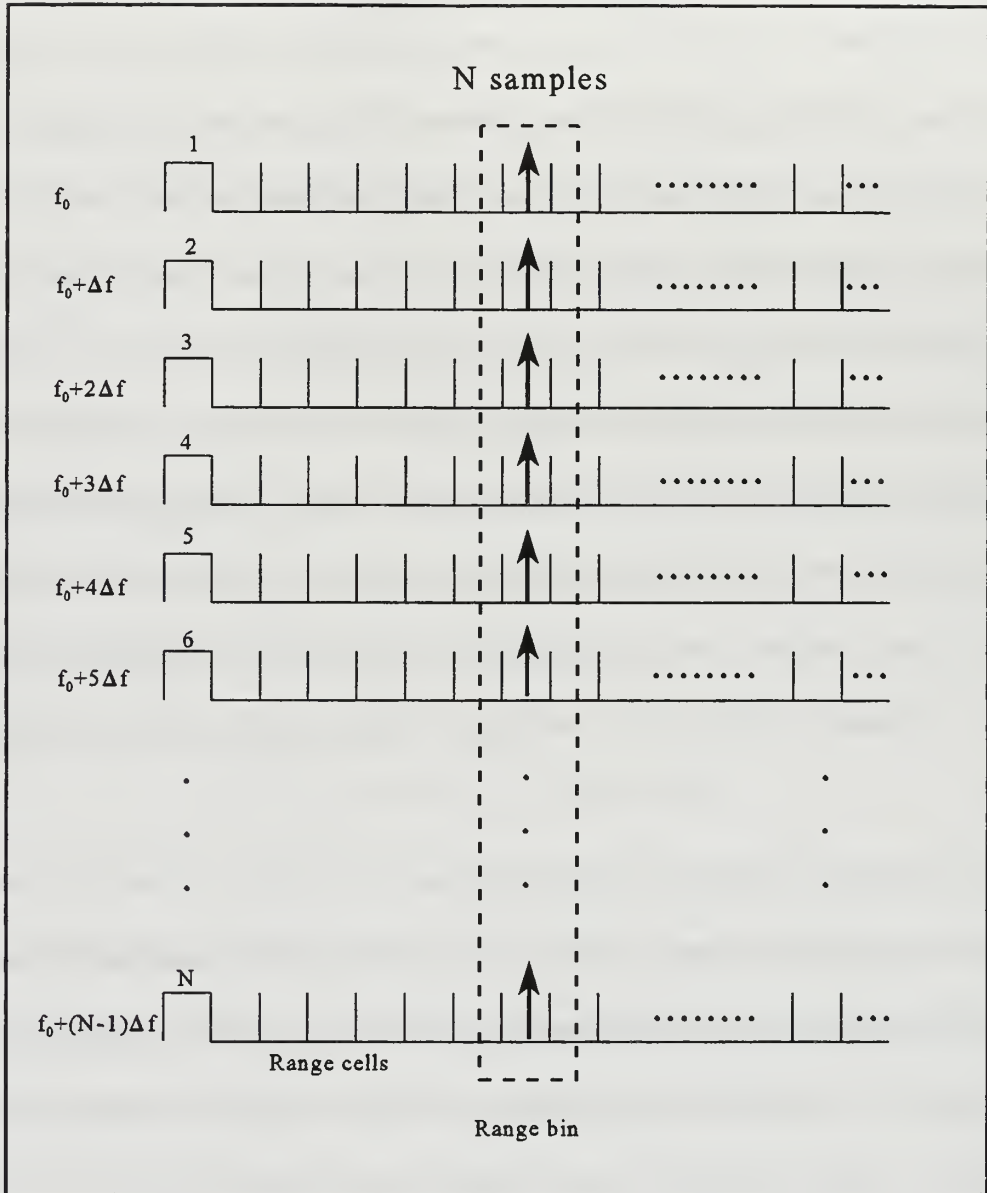
Figure 3.   N samples from a target are collected and stored in memory for processing.

C. WAVEFORM PROCESSING

The radar return signal at the output of the coherent detector can be written as

$$s(n) = I(n) + jQ(n) = A_n \exp(j\phi_n) , \qquad (2.7)$$

where

A_n = the magnitude of the nth pulse;

ϕ_n = the phase of the nth pulse.

A_n represents an amplitude factor which depends on the transmitted power, the size of the target, its dielectric constant (relative to that of the medium where it is embedded), and the propagation losses in the medium. The signal components are shown in Figure 4.

$$I(n) = A_n \cos \phi_n$$

$$Q(n) = A_n \sin \phi_n$$
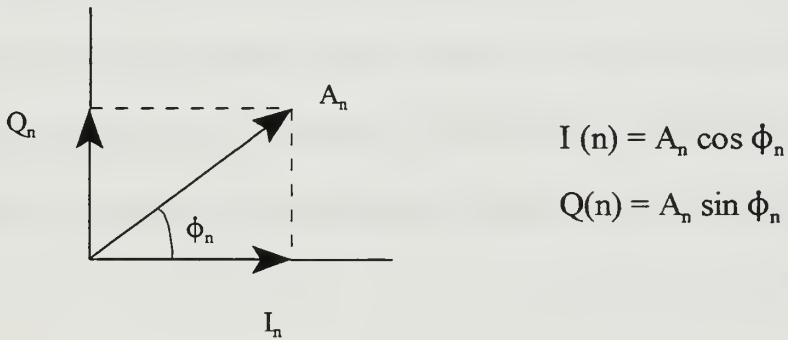
Figure 4.   Vector Representation of the Signal Components.

11

The phase of the nth pulse can be written as

$$\phi_n = 2\pi f_n t_r = 2\pi f_n \frac{2R_n}{c},$$

(2.8)

where f_n is the carrier frequency of the nth pulse and t_r is the round trip time from the target measured by the nth pulse. This time is equal to $2R_n/c$, with R_n being the range between the target and the radar. For a target with constant velocity toward the radar, the range R_n is given by

$$R_n = R_0 - (n-1)vT,$$

(2.9)

where

$R_0 =$ initial target range;

$T =$ pulse repetition interval;

$v =$ relative radial velocity between target and radar.

The overall expression for the baseband return signal can now be determined by substituting the instantaneous frequency from Equation 2.1, and the target range from Equation 2.9 in Equation 2.8, and then substituting the resulting expression in Equation 2.7. The resulting equation is as follows:

$$s(n) = A_n \exp\left[j\frac{4\pi}{c} f_n R_n\right]$$

$$= A_n \exp\left[j\frac{4\pi}{c} \left(f_0 + (n-1)\Delta f\right)\left(R_0 - (n-1)vT\right)\right].$$

(2.10)

The set of N sampled baseband signals s(n) from a given range bin is converted to the time domain range profile by taking the FFT;

$$H_k = \frac{1}{N} \sum_{n=1}^{N} s(n) \, \exp\left(j\frac{2\pi kn}{N}\right) \, , \qquad with \quad 0 \le k \le N-1. \tag{2.11}$$

III. STEP FREQUENCY WAVEFORM DESIGN

A radar can be classified as low PRF, high PRF or medium PRF. A low PRF is, by definition, one for which the maximum range the radar is designed to handle lies in the first range zone - the zone from which first-time-around echoes are received. Range for low PRF is unambiguous and doppler frequency is ambiguous. A high PRF is one for which the observed doppler frequencies of all significant targets are unambiguous and range is ambiguous. Finally, a medium PRF is one for which neither of these conditions is satisfied. Both range and doppler frequency are ambiguous. In this thesis the interest is the high PRF radar.

The purpose of this chapter is to develop a design procedure for detection of small targets with a surface (land or sea) based step frequency radar which employs a high PRF waveform. The disadvantage of high PRF is that the range ambiguity has to be resolved. However, several advantages result from high PRF. The unambiguous doppler leads to advantages such as elimination of clutter and absence or minimization of the blind doppler problem. It also improves the signal-to-noise (S/N) ratio by integration of larger number of pulses. For a constant frequency high PRF waveform, multiple time around clutter (from ambiguous regions due to different pulses) adds up and thus decreases the signal-to-clutter (S/C) ratio and increases the dynamic range of the receiver and associated A/D. Though the S/C ratio can be improved by doppler filtering, receiver and A/D will still require a large dynamic range as a large magnitude of folded clutter has to be accommodated in the receiver and A/D. The step frequency waveform reduces the folded clutter and thus the dynamic range by decreasing the number of range ambiguities. Range ambiguities in the step frequency

waveform depend upon the number of pulses which will pass through the IF filter simultaneously. This number is given by $1/(\tau\Delta f)$. By proper choice of the product $\tau\Delta f$, range ambiguities and thus clutter and dynamic range can be reduced. However, this advantage comes about at the cost of limiting the range coverage. This feature of the step frequency waveform provides a good tradeoff as high resolution radars are often limited by A/D technology. The waveform design involves the selection of PRF (f_r), number of pulses (N), frequency step (Δf) and pulse width (τ). It is assumed that the following radar performance related parameters are available: range resolution (ΔR), nominal carrier frequency (f_0), time-on-target (tot), minimum and maximum radial velocity (v_{min} and v_{max}) and the maximum number of pulses (N_{max}). The design of constant frequency waveforms is relatively simple and well documented. However, the design of step frequency waveforms is complex due to the conflicting effect of waveform parameters on various desired performance goals. Thus, in this chapter effort is made to systematize the design process for the high PRF step frequency waveform. The main point behind the design of high PRF waveforms is to keep the target in clutter free area and the target doppler unambiguous. This involves selection of PRF based on minimum and maximum target velocities and other parameters. PRF should be large enough that target at maximum expected velocity stays unambiguous in doppler. The other constraint is based on the fact that target doppler from minimum target velocity exceeds the clutter doppler. These constrains along with resolution requirements lead to the high PRF waveform design.

In this chapter, the method used to compute the desired parameters for the high PRF design case will be explained, but first two parameters will be defined and the expression for constraints on PRF will be derived.

1.   Definition of two constants

A dimensionless parameter P that relates the radial target motion over the time duration of the step frequency waveform to the resolution of the profile can be defined as:

$$P = \frac{vNT}{\Delta R},$$ (3.1)

where:

v = the radial velocity between the radar and the target (closing velocity);

NT = the duration of the step frequency waveform;

ΔR = the processed range resolution.

This is the ratio of how far the target moved with respect to the range resolution cell during the integration time. For all velocities with magnitude greater than zero, this represents a mismatch in the DFT (which acts like a matched filter), resulting in attenuation and dispersion of the HRR profile. In addition to the attenuation and dispersion that will result in a reduction in range resolution and S/N ratio, the uncompensated radial velocity will shift the HRR profiles by L FFT bins, where L is given by:

$$L = \frac{f_0}{B} P,$$ (3.2)

where:

f_0 = the nominal transmitter frequency (center frequency);

B = the total processed bandwidth.

2. Derivation of PRF constraints

To get a moving target in clutter free zone after DFT processing, the motion induced doppler shift should be such that shift L exceeds the clutter extent,

$$L \geq N\tau\Delta f. \tag{3.3}$$

From Equations 3.1, 3.2 and 3.3

$$\frac{2NTv}{\lambda} \geq N\tau\Delta f. \tag{3.4}$$

From above v_{min} is obtained as

$$\begin{aligned} v_{min} &= \frac{\lambda}{2T}\tau\Delta f \\ &= \frac{\lambda}{2T}\tau\frac{c}{2N\Delta R} \\ &= \frac{\lambda}{2T}\frac{c\tau}{2N}\frac{1}{\Delta R}. \end{aligned} \tag{3.5}$$

The constraint for maximum velocity can be derived by considering the worst case scenario for a target located at the end of the range gate (of width $c\tau/2$) at the maximum speed. To keep the doppler unambiguous, doppler shift and spread together should not exceed the PRF and therefore

$$L+P < N - N\tau\Delta f. \tag{3.6}$$

Substituting the value of L and P into this last equation,

$$\frac{2NTv}{\lambda} + \frac{vNT}{\Delta R} < N(1 - \tau \Delta f)$$

$$\frac{2Tv}{\lambda} + \frac{vT}{\Delta R} < 1 - \tau \Delta f \tag{3.7}$$

$$v + \frac{vT}{\Delta R}\frac{\lambda}{2T} < \frac{\lambda}{2T} - \tau \Delta f \frac{\lambda}{2T} \ .$$

Last term in right hand side of above equation can be recognized as the minimum velocity from Equation 3.5 and therefore

$$v\left(1 + \frac{\lambda}{2\Delta R}\right) < \frac{\lambda}{2T} - v_{min}$$

$$v_{max}\left(1 + \frac{\lambda}{2\Delta R}\right) + v_{min} \leq \frac{\lambda}{2T} = \frac{\lambda}{2}f_r \ . \tag{3.8}$$

Now, solving for f_r:

$$f_r \geq \frac{2}{\lambda}\left[v_{max}\left(1 + \frac{\lambda}{2\Delta R}\right) + v_{min}\right]. \tag{3.9}$$

Equality will give the minimum PRF ($f_{r\ min}$). If the factor $\lambda/(2\Delta R) << 1$, then the previous equation can be reduced to

$$f_r \geq \frac{2}{\lambda}\left[v_{max} + v_{min}\right]. \tag{3.10}$$

3.   Design Method

The initial specifications are the nominal carrier frequency (f_0), range resolution (ΔR), maximum radial velocity (v_{max}), minimum radial velocity (v_{min}), time on target (*tot*) and due

to processing constraints, the maximum number of pulses (N_{max}). The waveform parameters that we want to calculate are the PRF (f_r), number of pulses (N), frequency step size (Δf) and the pulse width (τ).

The proposed method consists of five steps, as follows:

1. Selection of PRF from given equation . This equation gives the minimum PRF and the exact value can be determined using an iterative procedure later.

2. The number of pulses is determined from *tot* and f_r :

$$N \geq (tot)\, f_r \;\; = \left(\frac{\theta_B}{\dot{\theta}_S} \right) f_r ,$$

(3.11)

where θ_B is the antenna beamwidth and $\dot{\theta}_S$ is the scan rate.

3. The frequency step size is calculated from

$$\Delta f = \frac{c}{2\, N \Delta R} ,$$

(3.12)

where c is the speed of light (3×10^8 m/sec).

4. The pulse width is chosen from Equation 3.5, which can be rewritten as

$$\tau \leq \frac{2}{\lambda} \frac{v_{min}}{f_r\, \Delta f} .$$

(3.13)

N and τ will impact the S/N ratio which determines the radar performance, that is probability of detection and probability of false alarm for given radar parameters. Therefore it should be ascertained from the following equation that chosen N and τ yield adequate S/N

ratio to satisfy the radar performance requirements.

$$\frac{S}{N} = \frac{P_t G^2 \lambda^2 \sigma (\tau N)}{(4\pi)^3 R^4 k T_0 F L},$$ (3.14)

where

P_t = the transmitted peak power (watts);

G = the antenna gain of the transmitter/receiver;

λ = the wavelength (meters);

σ = the radar cross section of the target (square meters);

τ = the pulse width (meters);

N = the number of pulses coherently integrated within one scan;

R = the detection range of the target (meters);

k = Boltzmann's constant (1.38×10^{-23} watt-second/°K);

T_0 = the noise temperature (°K);

F = the receiver noise figure;

L = a loss factor incorporating all system losses.

By convention, T_0 is taken to be 290°K, which is close to room temperature (300°K)

and conveniently makes the product $k T_0$ a round number (4×10^{-21} watt-second/°K).

5. Flexibility in PRF constraint can be used to satisfy other design objectives such as

the search range;

$$\text{Search range} = \text{number of } R_u\text{'s} \cdot R_u$$

$$= \frac{B_{IF}}{\Delta f} R_u$$

$$= \frac{k/\tau}{\Delta f} R_u \quad\quad\quad (3.15)$$

$$= \frac{k}{\tau \Delta f} \frac{c}{2 \Delta f}.$$

where R_u is the unambiguous range and B_{IF} is the intermediate frequency bandwidth. N, f_r, τ and Δf are changed iteratively such that the required search range is obtained. Extent of R_u should not increase clutter as range resolution is already fixed. However the number of R_u's will increase clutter (which should not matter if cancellation is adequate).

The initial specifications and the final calculated design parameters can be summarized in the following table:

Specifications	Calculated Design Parameters
Range resolution (ΔR)	Minimum PRF (f_r)
Nominal carrier frequency (f_0)	Number of pulses (N)
Time-on-target (tot)	Frequency step size (Δf)
Minimum radial velocity (v_{min})	Pulse width (τ)
Maximum radial velocity (v_{max})	
Maximum number of pulses (N_{max})	

Table 1. Summary of specifications and design parameters.

4.   Graphical implementation of the Design Method

Using the equations mentioned in the previous section, a graphical method to design the waveform was developed. The first graph is a plot of the range resolution versus minimum PRF, for four different nominal carrier frequencies.
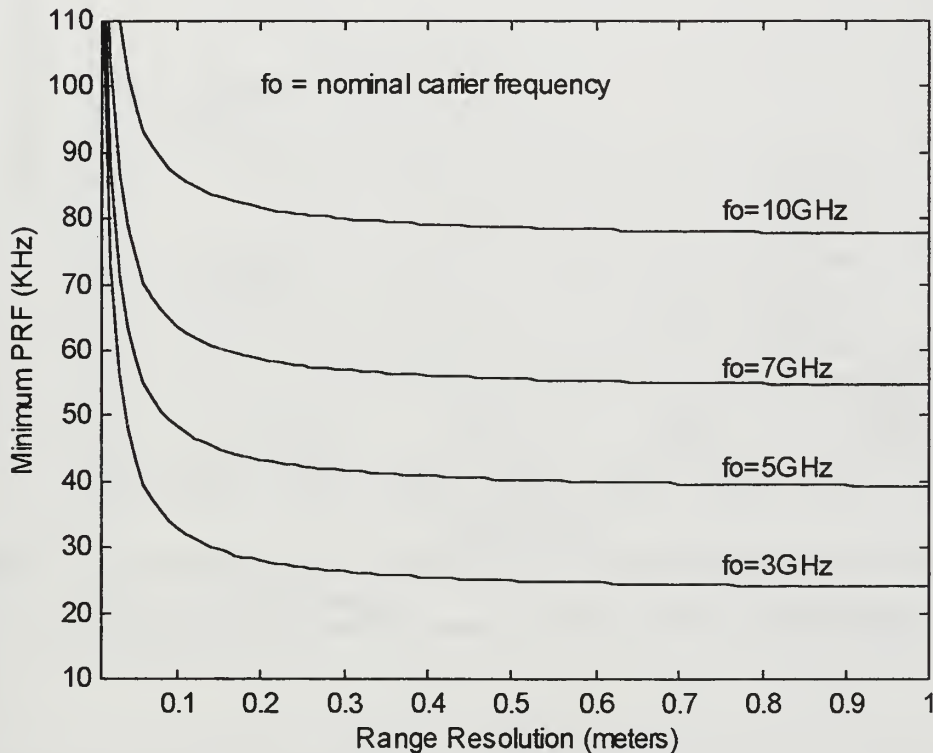
Figure 5.   Minimum PRF versus range resolution for four different nominal carrier frequencies.

This graph was created using Equation 3.9 and it can be observed that as the value of the desired range resolution decreases (corresponding to an improvement in the range resolution), the minimum PRF increases. This graph is used to determine the PRF for a given range resolution and carrier frequency.

23

The next graph, Figure 6, is a plot of the PRF versus the number of pulses, and was generated using Equation 3.11.
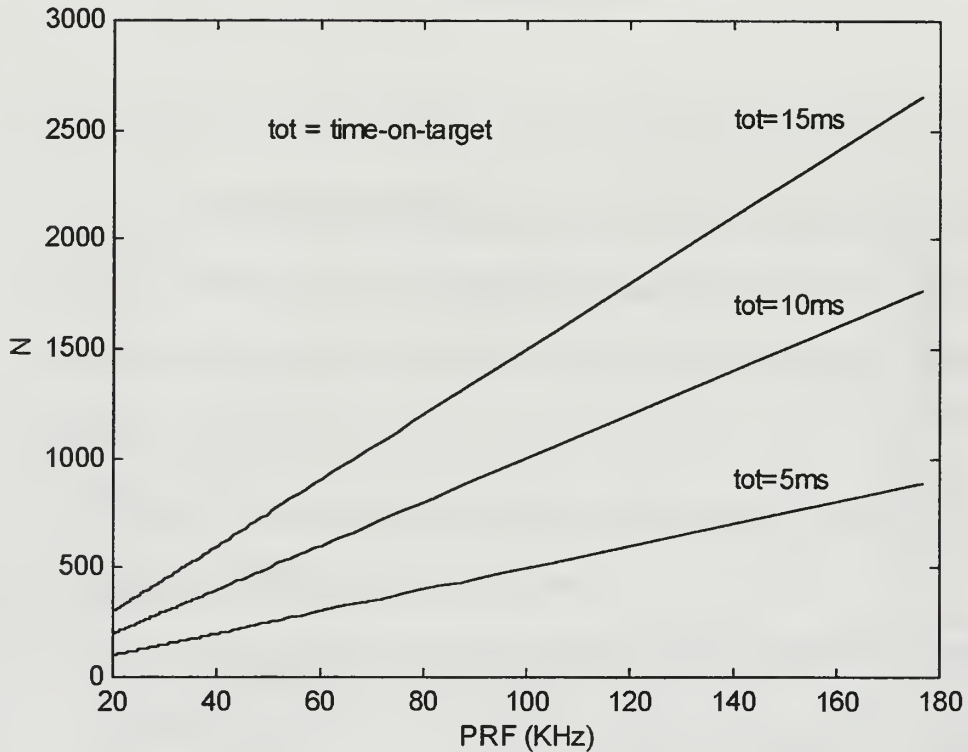
Figure 6.   Number of pulses versus PRF for three different times-on-target (5, 10, and 15 ms).

This plot is used to determine the number of pulses for a given time-on-target (tot) and PRF, computed in the previous step from Figure 5. Then, and using Equation 3.12, the frequency step size was plotted versus the number of pulses, for three different values of range resolution (0.3, 0.5, and 1 meter) as can be observed in Figure 7. This graph is used to determine the frequency step for a given range resolution and number of pulses computed in the previous step from Figure 6. The frequency step size required for the same number of

pulses increases as the desired range resolution decreases. Therefore, the better range resolution is desired, the higher the frequency step size must be.
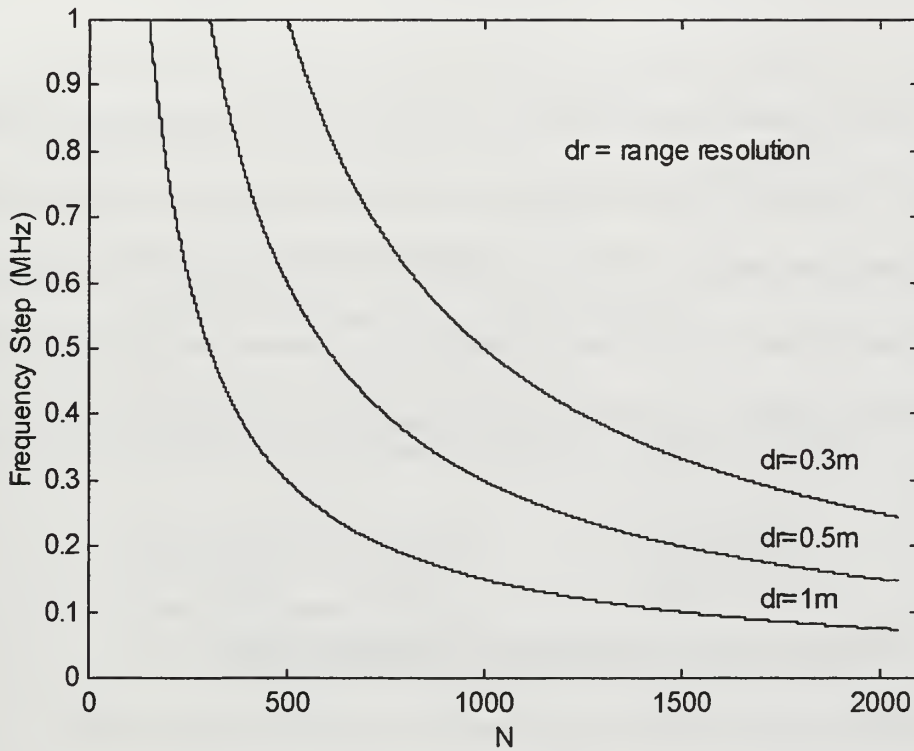
Figure 7.   Frequency step versus number of pulses for three different range resolutions (0.3, 0.5, and 1 meter).

Finally, the last step is to compute the pulse width using Equation 3.13, and all the calculated design parameters from Table 1 will be obtained.

Note that in all the calculations and plots above described v_{min} was considered to be 150 m/s and v_{max}, 1000 m/s. The value considered for N_{max} was 2048.

Consider an example to determine the design parameters for a step frequency radar with a nominal carrier frequency of 10 GHz, time-on-target of 15 ms and a desired range resolution of 0.3 m. From Figure 5 a minimum PRF of 80 KHz would be obtained. Using this

value and Figure 6, N would be approximately equal to 1200. Now with N=1200, dr=0.3m and using Figure 7, the frequency step would be approximately 0.42 MHz. The last step is to compute the value of the pulse width using Equation 3.14 and the result would came up to be τ=298 ns.

Interpolation should be used in this plots whenever the specifications are different from the values in the plots. However some times the desired values are beyond the plotted values. Additionally, not only we want to compute the desired parameters that satisfy the initial specifications, but also we may want to satisfy some parameter constraints. Therefore a MATLAB code was written in order to fulfill this requirement. This program can be found in Appendix B.

5. Computer implementation of the Design Method

The waveform design parameters are constrained to the following values:

- Pulse width - between 50 nsec and 5000 nsec

- Frequency step - should be 0.4, 0.6, 0.8 or 1 MHz

- PRF - should be an integer multiple of 5 KHz

The program is written in a way so that it will ask for the desired range resolution, nominal carrier frequency, and the time-on-target and these data should be entered from the keyboard. With this input data the program will compute the minimum values using the equations previously presented. These values are iterated until the constraints mentioned above are all satisfied and the desired design parameters obtained. The minimum values are shown in brackets. The program will also compute the actual range resolution and time-on-target corresponding to the rounded values of the PRF, frequency step, pulse width and number of

pulses. Figure 8 illustrates how the screen will appear.

Enter the desired range resolution in meters : 0.3

Enter the nominal carrier frequency in GHz : 10

Enter the time-on-target in msec : 15

The calculated design parameters are :   (minimum values)

- PRF = 140.00 KHz   (80.00 KHz)
- Frequency step = 0.40 MHz   (0.42 MHz)
- Pulse width = 180.00 nsec   (300.00 nsec)
- Number of pulses = 2048   (1200)
- Actual range resolution = 0.19 m
- Actual time-on-target = 14.63 msec

Figure 8. Example of the screen when running *program2.m* .

IV.   STEP FREQUENCY WAVEFORM ANALYSIS USING THE AMBIGUITY FUNCTION

A.   INTRODUCTION

In this chapter, the ambiguity function for a specific step frequency waveform will be determined. The waveform with the following parameters is of practical interest:

$$t_s = 0.1 \ \mu sec,$$

$$T = 5 \ \mu sec,$$

$$\Delta f = 1 \ MHz,$$

$$N = 500,$$

where t_s is the pulse width, T is the PRI, Δf is the frequency step, and N is the number of pulses. However, it is difficult to compute and plot this ambiguity function with the desired resolution because of the very large amount of computations involved. Not only the amount of computations is large but also the plotting is hard to handle because the files can easily reach several megabytes. Therefore, waveforms with parameters similar to the waveform of interest but easier to compute will be investigated, to bring out the key characteristics of the waveform under investigation. First, theoretical dimensions will be verified with a few cases. Then, these theoretical dimensions will be used for a particular case of interest which is difficult to compute directly.

Since the ambiguity function of the step frequency waveform contains elements of ambiguity functions of linear frequency modulated (LFM) pulses and train of constant frequency pulses, the ambiguity functions of these waveforms will be introduced first, along with the general introduction to ambiguity function.

B. DEFINITION OF AMBIGUITY FUNCTION AND ITS PROPERTIES

1. Definition of Ambiguity Function

A radar waveform's ambiguity function is probably the most complete statement of the waveform's inherent performance. It is a formula that quantitatively describes the interference caused by a point target return located at a different range and velocity from a reference target of interest. It reveals the range-doppler position of ambiguous responses and defines the range and doppler resolution. [Ref. 2, pp. 74]

This quantitative description of the ability of a waveform to resolve two or more radar reflectors at arbitrarily different ranges and velocities, constitutes an important feature for quick assessment of the interference level with which a target of interest must compete when it is in the vicinity of the other radar reflectors. Although it is seldom used as a basis for practical radar system design, it provides an indication of the limitations and utility of particular classes of radar waveforms, and gives the radar designer general guidelines for the selection of suitable waveforms for various applications.

The ambiguity function of the waveform $s(t)$ can be defined in terms of the cross-correlation of a doppler-shifted version of the waveform, that is $s(t) \exp(j2\pi f_d t)$ with the unshifted waveform. Using the definition of cross-correlation, it follows that

$$\chi(\tau, f_d) = \int_{-\infty}^{+\infty} \left[s(t) e^{j2\pi f_d t} \right] \left[s^*(t-\tau) \right] dt \, , \tag{4.1}$$

where τ is the delay time and f_d is the doppler frequency shift. Rearranging the terms in the integral produces a common form of the ambiguity function as shown in Equation 4.2.

$$|\chi(\tau, f_d)| = \left| \int_{-\infty}^{+\infty} s(t)\, s^*(t-\tau)\, e^{j2\pi f_d t}\, dt \right| . \qquad (4.2)$$

A normalized expression is obtained by requiring that

$$\int_{-\infty}^{+\infty} |s(t)|^2 dt = 1 . \qquad (4.3)$$

With this normalization, the magnitude of the ambiguity function has a value of unity at the

origin.

2.   Properties of the Ambiguity Function

The ambiguity function has the following properties:

$$\text{Peak value of } |\chi(\tau, f_d)| = |\chi(0,0)| = E , \qquad (4.4)$$

$$|\chi(-\tau, -f_d)| = |\chi(\tau, f_d)| , \qquad (4.5)$$

$$|\chi(\tau, 0)| = \left| \int_{-\infty}^{+\infty} s(t)\, s^*(t-\tau)\, dt \right| , \qquad (4.6)$$

$$|\chi(0, f_d)| = \left| \int_{-\infty}^{+\infty} s^2(t)\, e^{j2\pi f_d t}\, dt \right| , \qquad (4.7)$$

$$\int_{-\infty}^{+\infty} \int_{-\infty}^{+\infty} |\chi(\tau, f_d)|\, d\tau\, df_d = E . \qquad (4.8)$$

Equation 4.4, states that the peak value of the ambiguity function occurs at the origin and it

is equal to E, the energy contained in the echo signal. Equation 4.5 shows the ambiguity

31

function's symmetry. Equation 4.6 indicates that the ambiguity function along the time delay axis is the auto-correlation function of the complex envelope of the transmitted signal. Equation 4.7 states that along the frequency shift axis the ambiguity function is proportional to the spectrum of $s^2(t)$. Finally, Equation 4.8 states that the total volume under the ambiguity surface is a constant equal to E.

3.   Ambiguity Diagram

It is common to refer to $|\chi(\tau, f_d)|$ as the ambiguity surface of the waveform. The shape of this ambiguity surface depends entirely on the waveform parameters. The plot of the ambiguity surface is called *ambiguity diagram*. The ideal ambiguity diagram consists of a single spike of infinitesimal thickness at the origin and is zero everywhere else. The single center spike eliminates any ambiguities, and its infinitesimal thickness at the origin permits the frequency and the echo delay time to be determined simultaneously to an high degree of accuracy. It also permits the resolution of two targets no matter how close together they are on the ambiguity diagram. Naturally, this ideal diagram does not exist. The two reasons for this can be found in the properties: first, and accordingly with Equation 4.4, the maximum height of the ambiguity function is E and secondly the volume under the surface must be finite and equal to E, as stated by Equation 4.8. However, a reasonable approximation is given in Figure 9. This ambiguity function only has one peak and therefore does not cause any ambiguity. However the single peak might not be narrow enough to satisfy the requirements of accuracy and resolution. If the single central peak is made too narrow, it may cause other smaller peaks to occur in regions other than the origin, and therefore cause ambiguities. The requirements for accuracy and unambiguity are not always possible to satisfy simultaneously.
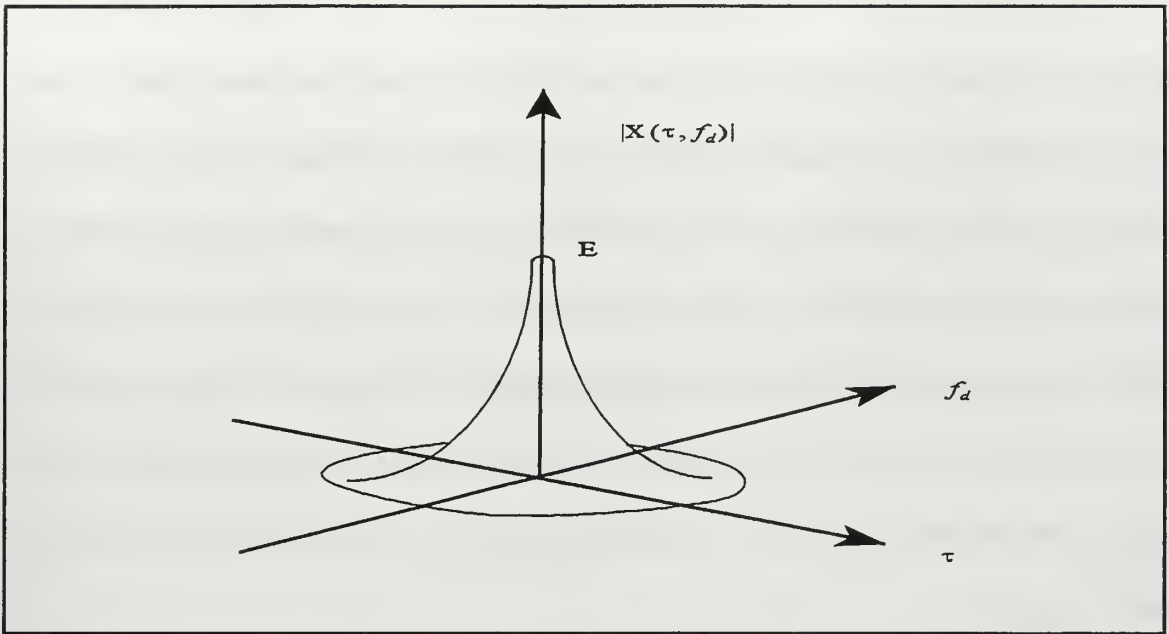
Figure 9. An approximation to the ideal ambiguity diagram "After Ref. [1]."

The particular waveform transmitted by a radar is chosen to satisfy the requirements for (1) detection, (2) measurement accuracy, (3) resolution, (4) ambiguity, and (5) clutter rejection. The ambiguity diagram may be used to assess how well a waveform can achieve these requirements. Each of these will be discussed briefly.

The requirements for *detection* do not place any demands on the shape of the transmitted waveform except that it be possible to achieve with practical radar transmitters, and the maximum value of the ambiguity function is an indication of the detection capabilities of the radar. The *accuracy* with which the range and the velocity can be measured by a particular waveform depends on the width of the central spike along the time and frequency axis. The *resolution* is also related to the width of the central spike, but in order to resolve two closely spaced targets the central spike must be isolated. It cannot have any high peaks nearby that can mask another target close to the desired target. A waveform that yields good resolution will also yield good accuracy, but the reverse is not always so.

A continuous waveform (a single pulse) produces an ambiguity diagram with a single peak. A discontinuous waveform can result in peaks in the ambiguity diagram at other values of τ, f_d. The pulse train is a common example. The presence of additional spikes can lead to *ambiguity* in the measurement of target parameters. An ambiguous measurement is one in which there are several choices available for the correct value of a parameter, but only one choice is appropriate. Thus the correct value is uncertain. The ambiguity diagram permits a visual indication of the ambiguities possible with a particular waveform. The ambiguity problem, detection and accuracy are related to a single target, whereas resolution applies to multiple targets.

The ambiguity diagram may be used to determine the ability of a waveform to reject clutter by superimposing on the τ, f_d plane the regions where clutter is found. If the transmitted waveform is to have good *clutter-rejection* properties the ambiguity function should have little or no response in the regions of clutter.

The problem of synthesizing optimum waveforms based on a desired ambiguity diagram specified by operational requirements is not normally feasible. The approach to selecting a waveform with a suitable ambiguity diagram is not systematic but rather by trial and error.

The name *ambiguity function* is somewhat misleading since this function describes more about the waveform than just its ambiguity properties. This name was given to this function in order to demonstrate that the total volume under it, is a constant equal to E, independent of the shape of the transmitted waveform. Thus the total area of ambiguity, or uncertainty, is the same no matter how the ambiguity surface is distributed over the τ, f_d plane. [Ref. 1, pp. 418-420]

C. AMBIGUITY FUNCTION OF A SINGLE PULSE

The unmodulated single pulse is widely used in old generation radars for search and track functions (as magnetrons are not easily modulated) and where range accuracy and resolution requirements can be met with a pulse wide enough to provide sufficient energy for detection. It has the minimum ratio of time sidelobe extent to compressed pulse width and is used in inexpensive radars where signal generation and processing costs must be minimized.

The single pulse of a sine wave can be defined as

$$S(t) = s(t)e^{j2\pi f_0 t} \quad , \tag{4.9}$$

where $s(t)$ is the complex envelope of the signal, defined as follows:

$$
\begin{aligned}
s(t) &= 1, \quad &\text{if } 0 \le t \le t_s, \\
&= 0, \quad &\text{elsewhere,}
\end{aligned}
\tag{4.10}
$$

with t_s equal to the pulse width.

Using Equation 4.2, the ambiguity function of the single pulse can be written as follows:

$$|\chi(\tau, f_d)| = \left| \int_\tau^{t_s} e^{j2\pi f_d t} dt \right|$$

$$= \left| \left(1 - \frac{|\tau|}{t_s}\right) \frac{\sin[\pi t_s(1-|\tau|/t_s)f_d]}{\pi t_s(1-|\tau|/t_s)f_d} \right| \quad , \quad \text{if } |\tau| \le t_s \;,$$

$$\text{zero elsewhere.} \tag{4.11}$$

The figures for this section are in Appendix A. The ambiguity diagram of the single pulse is shown in Figure A.1 and the contour plot can be observed in Figure A.2. Profiles of

the ambiguity function, taken through its peak, are shown in Figures A.3 and A.4. The time profile is a triangle (the autocorrelation of a rectangle is a triangle) with a half-voltage width equal to the pulse width. The frequency profile is a sinc function whose main lobe width is twice the reciprocal of the pulse width.

D.   AMBIGUITY FUNCTION OF THE LINEAR FREQUENCY MODULATED PULSE

The linear frequency modulated (LFM) pulse is commonly used to increase range accuracy and resolution when long pulses are required to get reasonable signal-to-noise ratios (10 to 20 dB). This waveform can be used for detection of targets with unknown velocity since the doppler sensitivity is low.

The LFM pulse can be represented mathematically as

$$S(t) = s(t) e^{j2\pi\left(f_0 t + \frac{1}{2}kt^2\right)}$$

$$= \left[s(t) e^{j\pi kt^2}\right] e^{j2\pi f_0 t} \quad ,$$

(4.12)

where $s(t)$ is the same as defined in Equation 4.10, and k is the rate of frequency change in Hz/sec. The ambiguity function of the LFM pulse can be written as in Equation 4.13.

$$|\chi(\tau, f_d)| = \left| \int_{-\infty}^{+\infty} s(t) \ s^*(t-\tau) \ e^{j2\pi(f_d - k\tau)t} dt \right|$$

$$= \left| \left(1 - \frac{|\tau|}{t_s}\right) \frac{\sin\left[\pi t_s (1 - |\tau|/t_s)(f_d + k\tau)\right]}{\pi t_s (1 - |\tau|/t_s)(f_d + k\tau)} \right| , \quad if \ |\tau| \le t_s,$$

zero elsewhere.   (4.13)

36

Comparing this equation with Equation 4.2, we can see that they are identical, except that f_d is replaced by $f_d - k\tau$. Therefore , we can conclude that the ambiguity function of the LFM pulse is a shifted version of the ambiguity function of a single pulse. This relation is represented graphically in Figure 10 and it can be seen that the ambiguity function of the LFM pulse is just a rotated version of the ambiguity function of the single pulse.
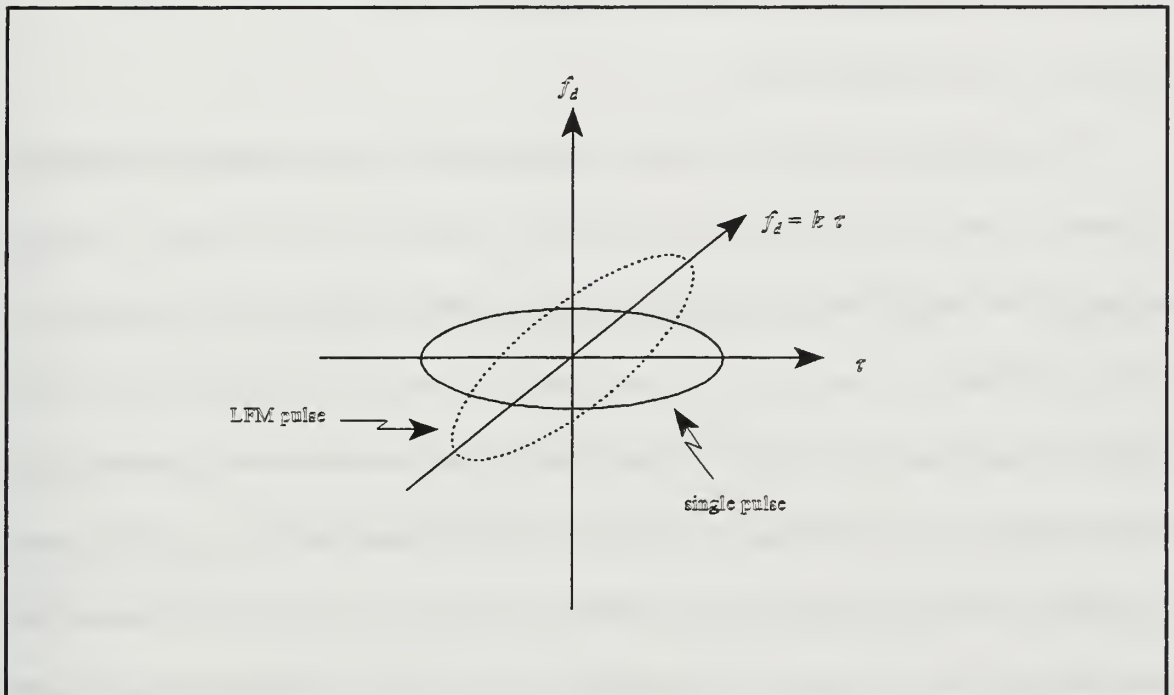

Figure 10. Contour comparison for the single pulse and the LFM pulse.

The figures for this section are in Appendix A. Figures A.5, A.6, A.7, and A.8, represent the ambiguity diagram, contour plot, and time and frequency profiles (taken through the peak), respectively.

E. AMBIGUITY FUNCTION OF THE CONSTANT FREQUENCY PULSE TRAIN

Practical radars employ waveforms consisting of constant frequency pulse trains and therefore it is important to study their ambiguity functions. The ambiguity functions for these pulse trains reveal ambiguous responses in range and doppler. Performance for specific surveillance applications can be understood in terms of unambiguous range-doppler regions of operation determined by radar pulse repetition frequency, pulse duration, and pulse bandwidth. For high resolution applications, the ambiguity surface of individual pulses of the pulse train is also of interest. [Ref. 2, pp. 74-75]

For single pulse delay and frequency measurement accuracies depend on the single parameter of pulse width. With the pulse train this situation can be avoided. The delay accuracy depends on the pulse width as before, but the frequency accuracy is now determined by the total duration of the pulse train. Therefore, both accuracies are independent of one another. The price that has to be paid for this capacity of independently controlling delay and frequency accuracies is that additional peaks occur in the diagram, which in turn cause range and doppler ambiguities. In practice, the radar designer tries to select the PRI in order to make all targets of interest appear in the vicinity of the central peak, and all the other peaks occur as far from this region as possible.

Most radars use this type of waveform, which can be mathematically represented as follows:

$$S(t) = \sum_{n=0}^{N-1} s(t-nT) \, e^{j2\pi f_0 t} \, , \tag{4.14}$$

where $s(t)$ is the complex envelope of the single pulse of the transmitted signal, defined as

$$s(t-nT) = 1, \qquad\qquad\text{if}\quad nT \le t \le nT + t_s \,,$$
$$= 0, \qquad\qquad\text{elsewhere.} \qquad\qquad (4.15)$$

In this equation, N is the number of pulses, T is the PRI and t_s is the pulse width. The ambiguity function of the constant frequency pulse train can be written as

$$|\chi(\tau,f_d)| = \left| \int_{-\infty}^{+\infty} \sum_{n=0}^{N-1} s(t-nT) \sum_{m=0}^{N-1} s^*(t-mT-\tau)\, e^{j2\pi f_d t}\, dt \right|. \qquad (4.16)$$

Changing variables ($t-nT=t'$), Equation 4.16 becomes

$$|\chi(\tau,f_d)| = \left| \sum_{n=0}^{N-1} \sum_{m=0}^{N-1} e^{j2\pi f_d nT} \int_{-\infty}^{+\infty} s(t')\, s^*(t'-(m-n)T-\tau)\, e^{j2\pi f_d t'}\, dt' \right|. \qquad (4.17)$$

Figure 11 is a level contour of the ambiguity surface of a constant frequency pulse train. This figure shows that the width of the central peak along the delay axis is approximately twice the pulse width, and that along the frequency axis is 2/NT. The interpeak distance along the delay axis is equal to the PRI, and along the frequency axis 1/PRI, which is the PRF of the waveform. The total non-zero extent along the delay axis is 2NT and along the frequency axis is 2/t_s. Figure 12 represents an example of an ambiguity diagram for the constant frequency pulse train. The contour plots in Figures 13 and 14 show that the results obtained agree with the theoretical ones previously defined. This can also be observed in Figures 15 and 16, which represent the time and frequency profiles, respectively. The time profile of the central pulse is a triangle and the frequency profile is a sinc function, as expected.
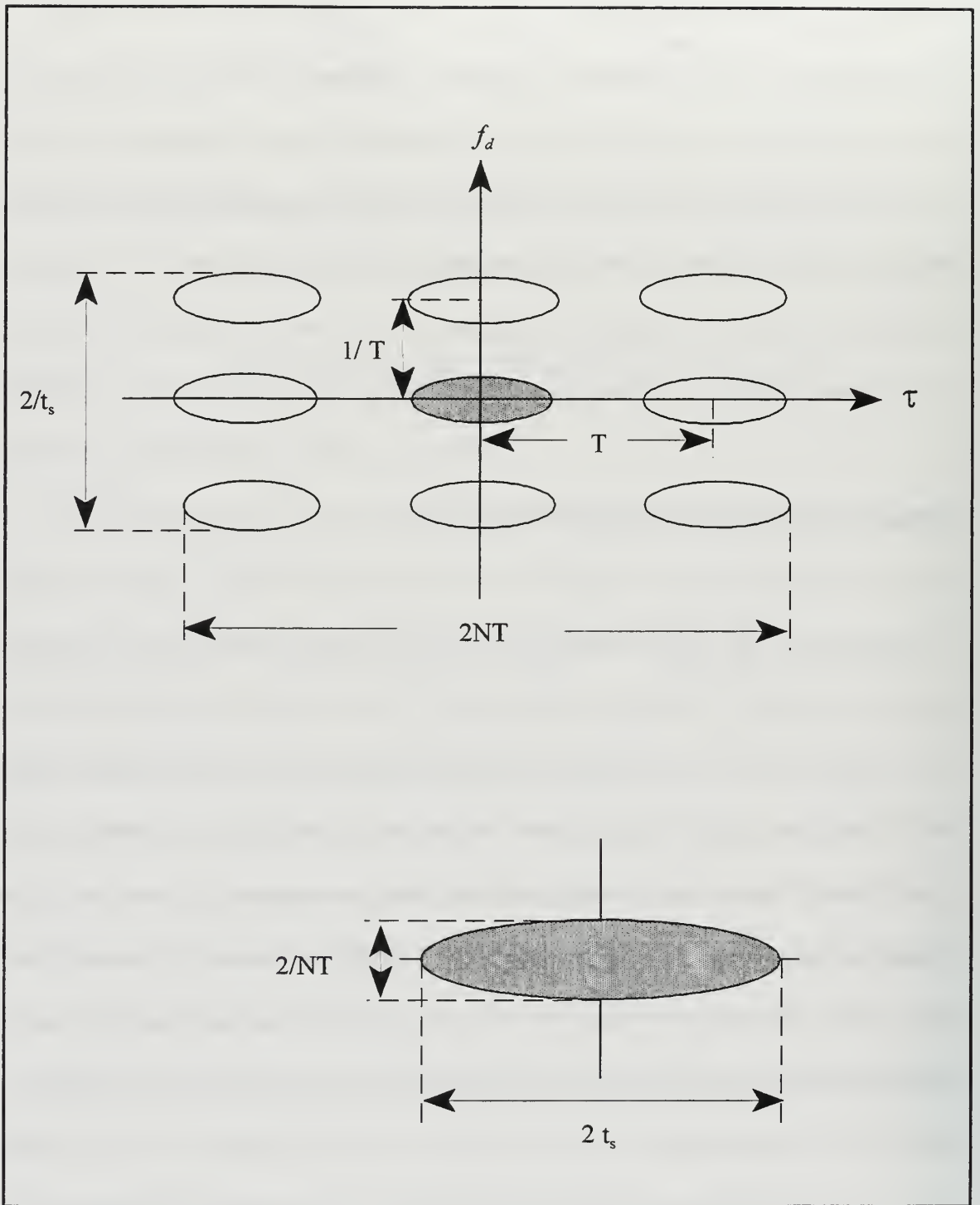
Figure 11. Level contour of the ambiguity surface of a constant frequency pulse train.
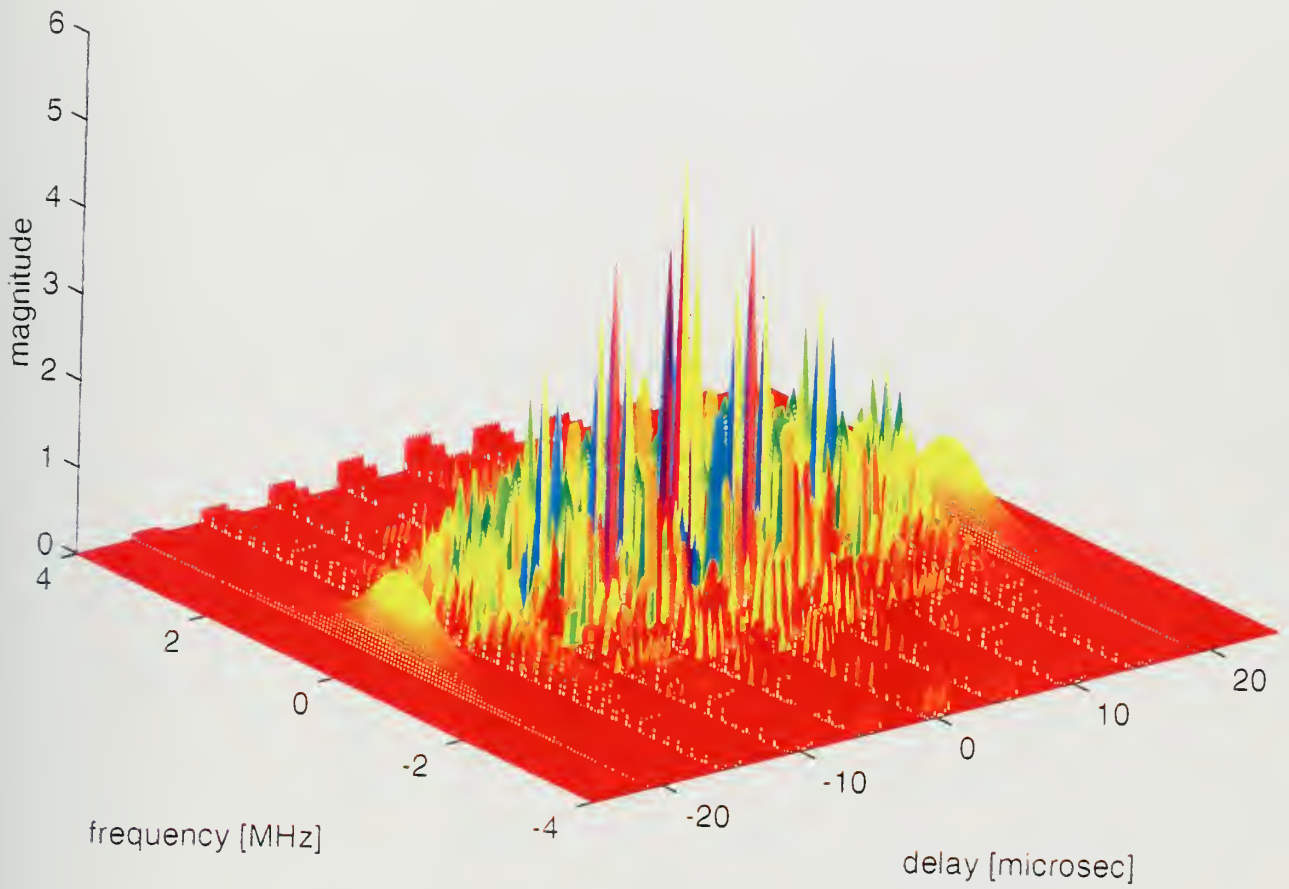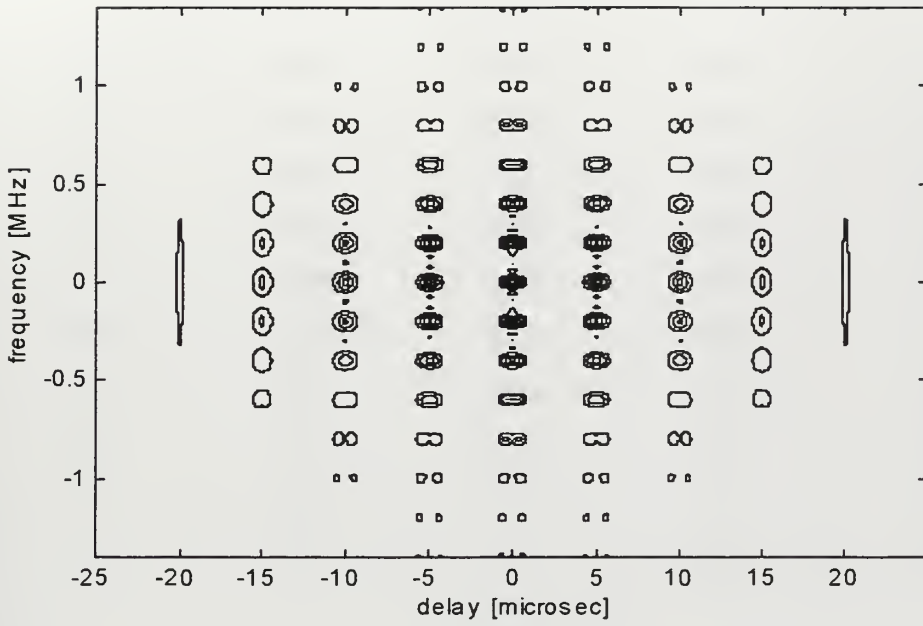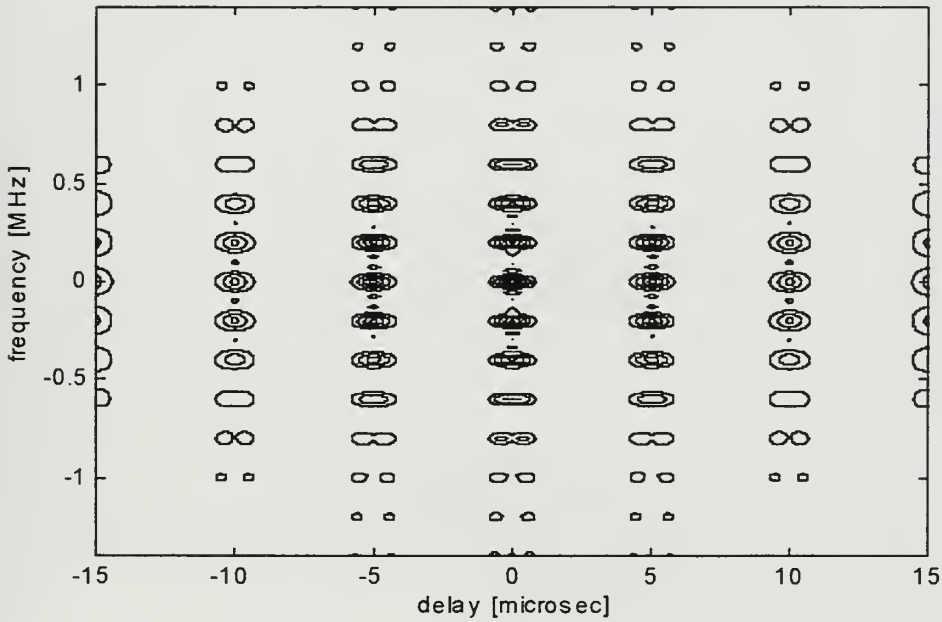
Figure 12. Ambiguity diagram of a constant frequency pulse train.
(N=5, pulse width=1 microsec, PRI=5 microsec, Δf=0)

Figure 13. Contour plots of the ambiguity diagram of a constant frequency pulse train.
(N=5, pulse width=1 microsec, PRI=5 microsec, Δf=0)
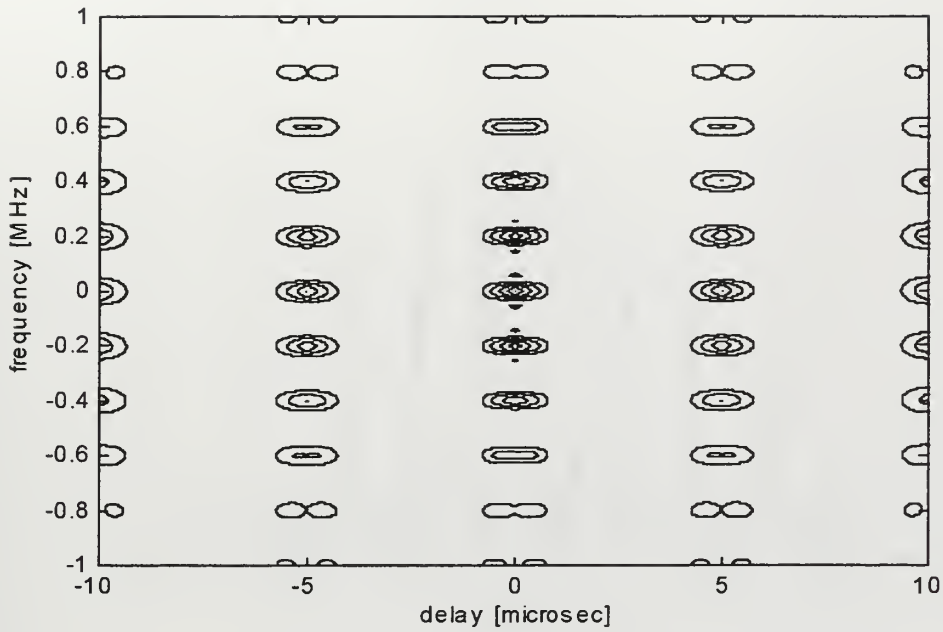(a) Global view.
(b) Magnified view.
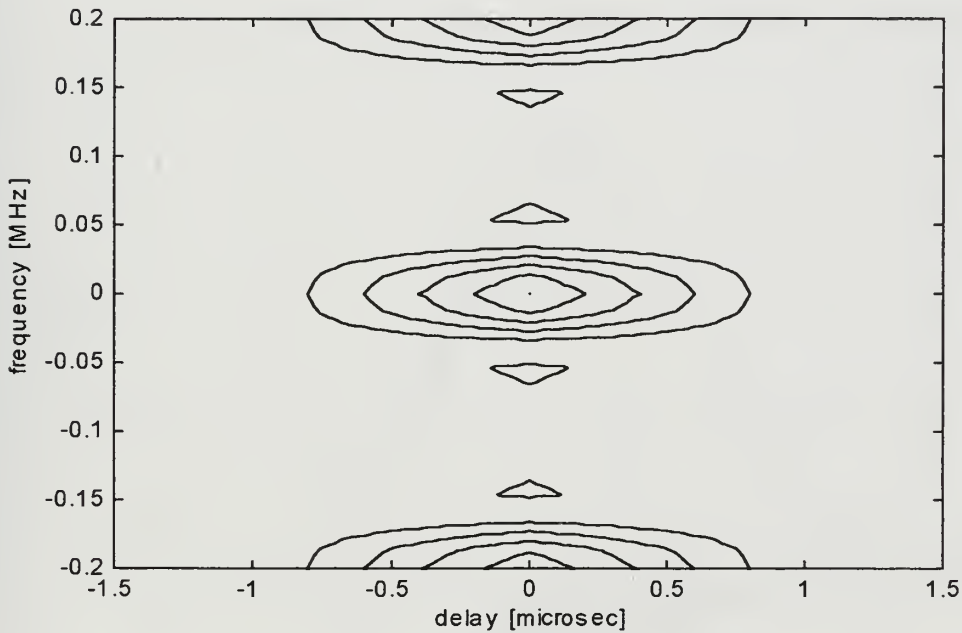
Figure 14. Contour plots of the ambiguity diagram of a constant frequency pulse train.
(N=5, pulse width =1 microsec, PRI=5 microsec, $\Delta f=0$)
(a) Magnified view.
(b) Magnified view of the central peak.

43

Figure 15. Time profiles of the ambiguity diagram of a constant frequency pulse train.
(N=5, pulse width =1 microsec, PRI=5 microsec, Δf=0)
(a) Global view.
(b) Magnified view.

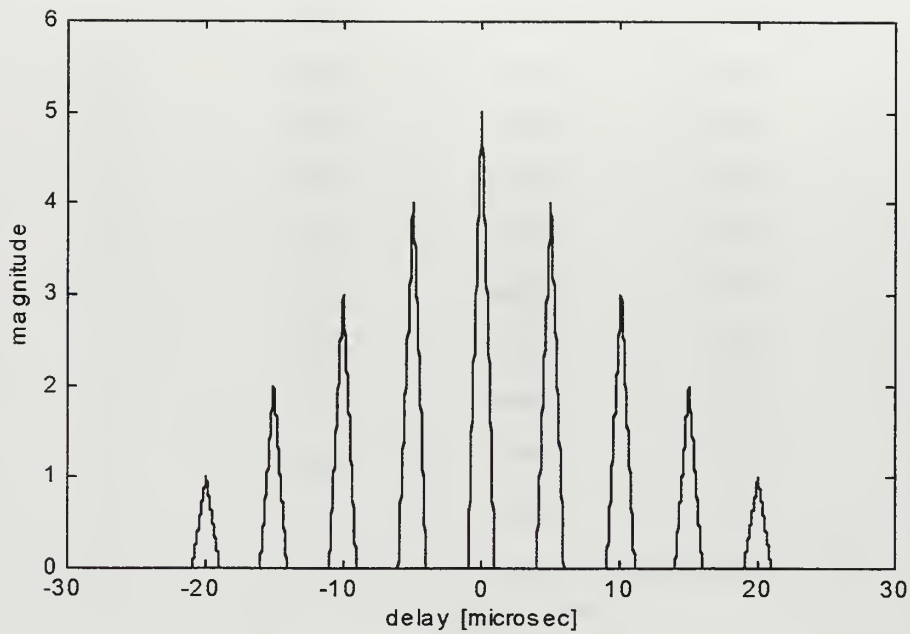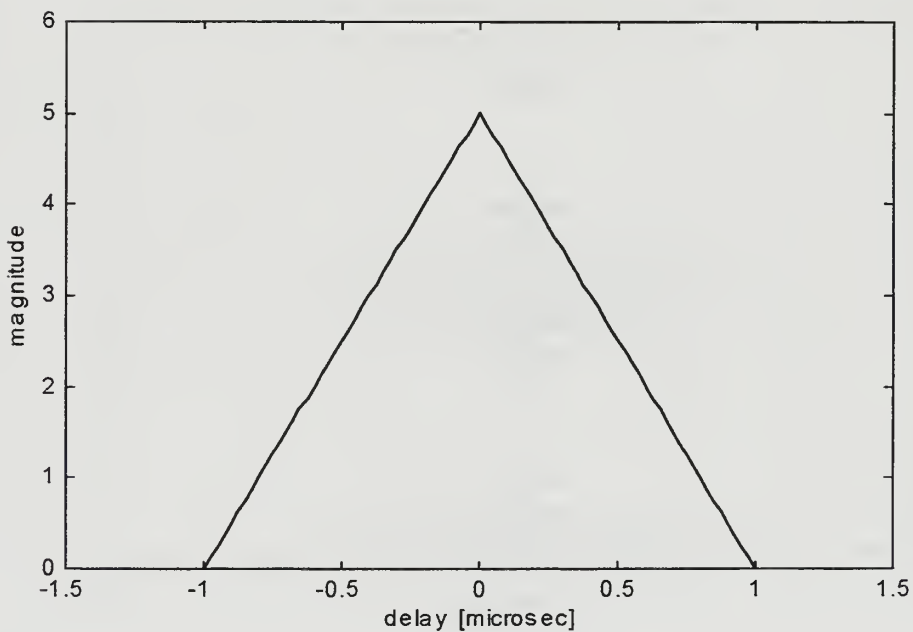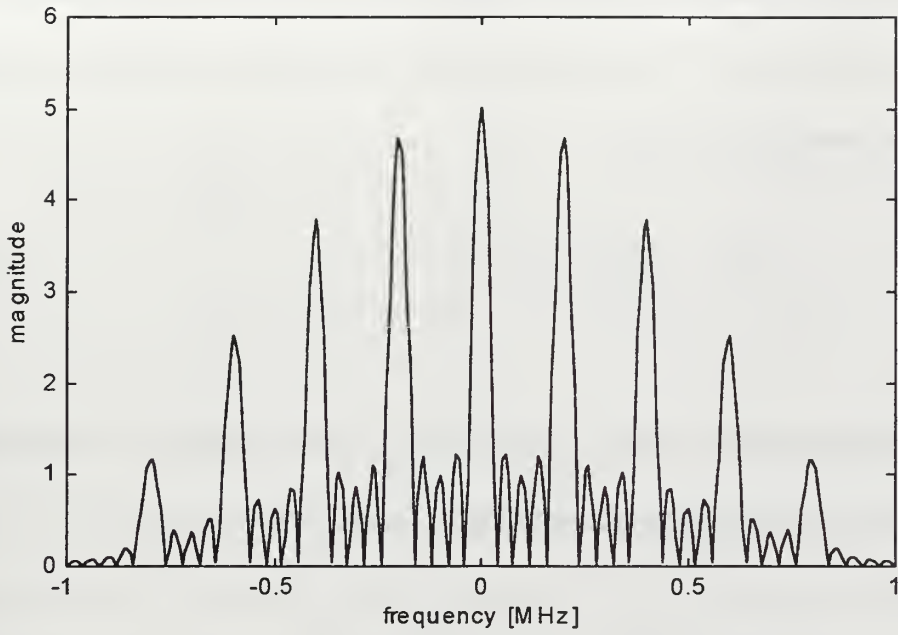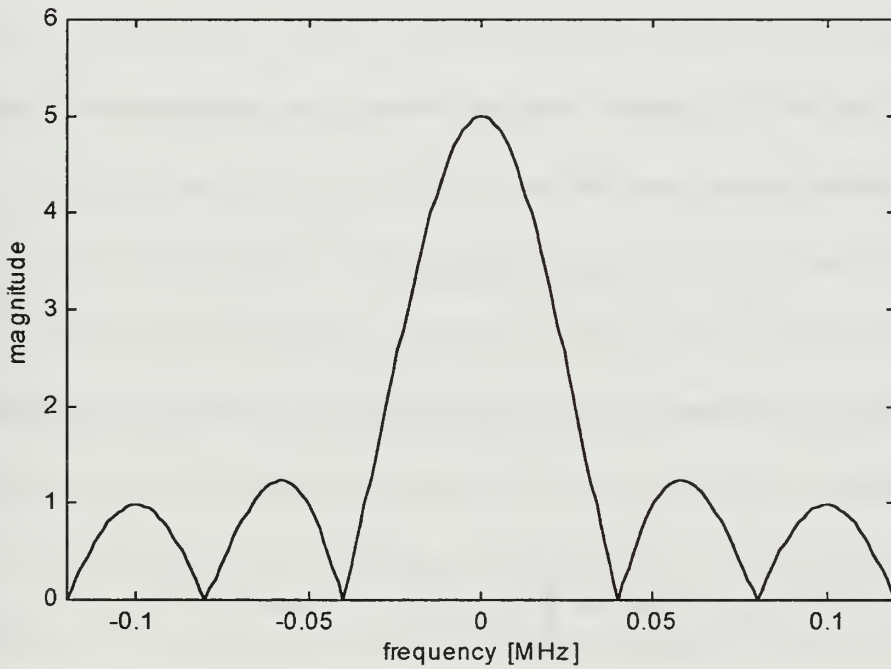Figure 16. Frequency profile of the ambiguity diagram of a constant frequency pulse train . (N=5, pulse width =1 microsec, PRI=5 microsec, Δf=0)
(a) Global view.
(b) Magnified view.

45

F. AMBIGUITY FUNCTION OF THE STEP FREQUENCY WAVEFORM

The transmitted signal of the step frequency radar (as shown in Figure 1) can be represented mathematically as follows:

$$S_t(t) = A_t \sum_{n=0}^{N-1} s(t-nT) \, e^{j2\pi(f_0+n\Delta f)t} \, ,$$

(4.18)

with $s(t)$ defined in Equation 4.15, and $n = 0, \ldots, N-1$. A_t is the amplitude of the transmitted signal. Equation 4.18 can be rewritten as follows:

$$S_t(t) = A_t \left[\sum_{n=0}^{N-1} s(t-nT) \, e^{j2\pi n\Delta f t} \right] e^{j2\pi f_0 t}$$

$$= A_t \, S(t) \, e^{j2\pi f_0 t} \, ,$$

(4.19)

The expression in brackets is the complex envelope of the pulse sequence represented by $S(t)$.

The received signal can be written as

$$S_r(t) = A_r \, S(t-\tau) \, e^{j2\pi(f_0+f_d)(t-\tau)} \, .$$

(4.20)

Substituting the complex envelope $S(t)$ into Equation 4.2, will give an expression for the ambiguity function

$$|\chi(\tau,f_d)| = \left| \int_{-\infty}^{+\infty} \left[\sum_{m=0}^{N-1} s(t-mT) \, e^{j2\pi m\Delta f t} \sum_{n=0}^{N-1} s^*(t-nT-\tau) \, e^{-j2\pi n\Delta f(t-\tau)} \right] e^{2\pi f_d t} \, dt \right| .$$

(4.21)

Changing variables ($t-mT = t'$), the final expression for the ambiguity function of the step frequency waveform is obtained:

$$|\chi(\tau, f_d)| = |\sum_{m=0}^{N-1} \sum_{n=0}^{N-1} e^{j2\pi m^2 \Delta f T} e^{j2\pi m f_d T} e^{-j2\pi m n \Delta f T} e^{j2\pi n \Delta f \tau}$$

$$\times \int_{-\infty}^{+\infty} s(t') \, s^*(t'-(n-m)T-\tau) \, e^{j2\pi(m-n)\Delta f t'} \, e^{j2\pi f_d t'} \, dt' | \; .$$

(4.22)

The theoretical dimensions of the contours of the ambiguity surface for the step frequency waveform are shown in Figure 17. The overall dimensions are of length 2NT along the delay axis and $2N\Delta f$ along the frequency axis. It can be observed that the distance between component contours along the delay axis is equal to the PRI of the waveform and along the frequency axis is equal to the inverse of the PRI. The ambiguity diagram of the step frequency waveform can be obtained from the ambiguity diagram of the constant frequency pulse train (same parameters), by rotating the delay axis by $\Delta f/T$. This can be stated more accurately by saying that the ambiguity function of the step frequency radar is $\chi(\tau, (\Delta f/T) f_d)$ where $\chi(\tau, f_d)$ is the ambiguity function of the constant frequency pulse train. Apart from rotation of horizontal axis (and all cuts parallel to it) the individual spikes also rotate. This is similar to linear frequency modulation pulses. The extent of the central column of spikes along the frequency axis for zero delay is $2/t_s$, value which decreases when we move away from the center. The central spike as shown in Figure 17 is inclined $\Delta f/T$ with respect to the horizontal axis, indicating the range-doppler coupling of the step frequency waveform. The projection of the central peak on the delay axis is $2t_s$, which is the overall delay uncertainty. However if the doppler is known, the delay uncertainty is given by $2/(N\Delta f)$ as indicated in the figure. The projection of the central peak on the frequency axis is also indicated in the figure. If the
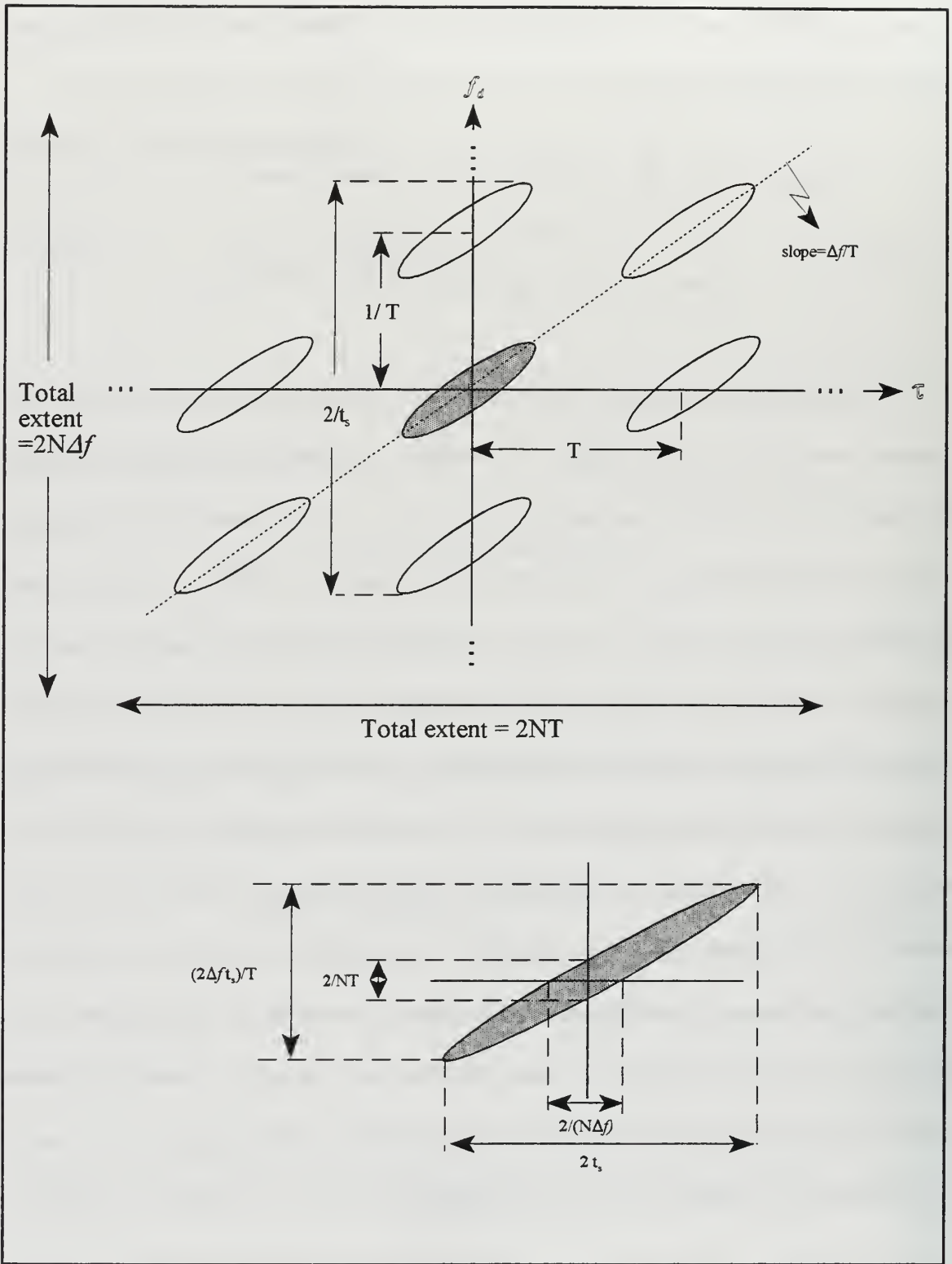
Figure 17.   Level contour of the ambiguity surface of a step frequency waveform.

delay is known, the frequency uncertainty is 2/NT which is the same as for the constant

frequency pulse train. However if target delay is not known, frequency uncertainty is much

larger due to range-doppler coupling.

G. AMBIGUITY FUNCTION OF STEP FREQUENCY WAVEFORMS

Four waveforms will be studied in this section. These waveforms are defined by the

following parameters:

1. N=5, t_s =1 µs, PRI =5 µs, Δf =1 MHz.

2. **N=10**, t_s =1 µs, PRI =5 µs, Δf =1 MHz.

3. N=10, **t_s =0.1 µs**, PRI =5 µs, Δf =1 MHz.

4. **N=500**, t_s =0.1 µs, PRI =5 µs, Δf =1 MHz.

1.   First waveform

The results for this waveform are shown in Figures 18 through 22. The ambiguity

diagram is represented in Figure 18. It can be observed that it is spiky like the one for the

constant frequency pulse train, but now it is tilted at an angle. The global view of the contour

plot of the ambiguity function for this waveform is shown in Figure 19(a). The rotation of the

plot with respect to the axes is obvious in the figure and the rotation angle is given by Δf/T.

The delay and frequency axis dimensions match the theoretical values as from -NT to NT and

from -NΔf to NΔf. Figure 19(b) is a close up view of the contour plot. Figure 20(a) is a

further magnification of the contour plot and Figure 20(b) shows the details of the central

peak. From the contour plot it is clear that the central peak is a inclined ridge with the highest

magnitude in the center of the contour. Figure 21(a) is a cut of the ambiguity surface along

Figure 18. Ambiguity diagram of a step frequency waveform
(N=5, pulse width=1 microsec, PRI=5 microsec, Δf=1MHz)
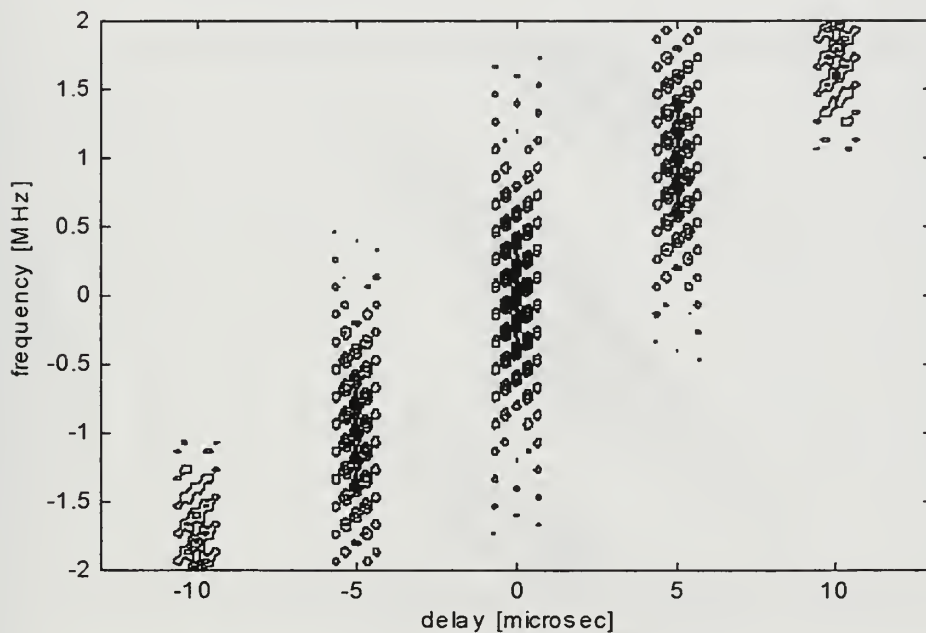
Figure 19. Contour plots of the ambiguity diagram of a step frequency waveform.
(N=5, pulse width=1 microsec, PRI=5 microsec, Δf=1 MHz)
(a) Global view.
(b) Magnified view.

(a)

(b)

Figure 20. Contour plots of the ambiguity diagram of a step frequency waveform.
(N=5, pulse width =1 microsec, PRI=5microsec, Δf=1 MHz)
(a) Magnified view.
(b) Magnified view of the central peak.

Figure 21. Time profiles of the ambiguity diagram of a step frequency waveform.
(N=5, pulse width =1 microsec, PRI=5 microsec, Δf=1MHz)
(a) Global view.
(b) Magnified view.

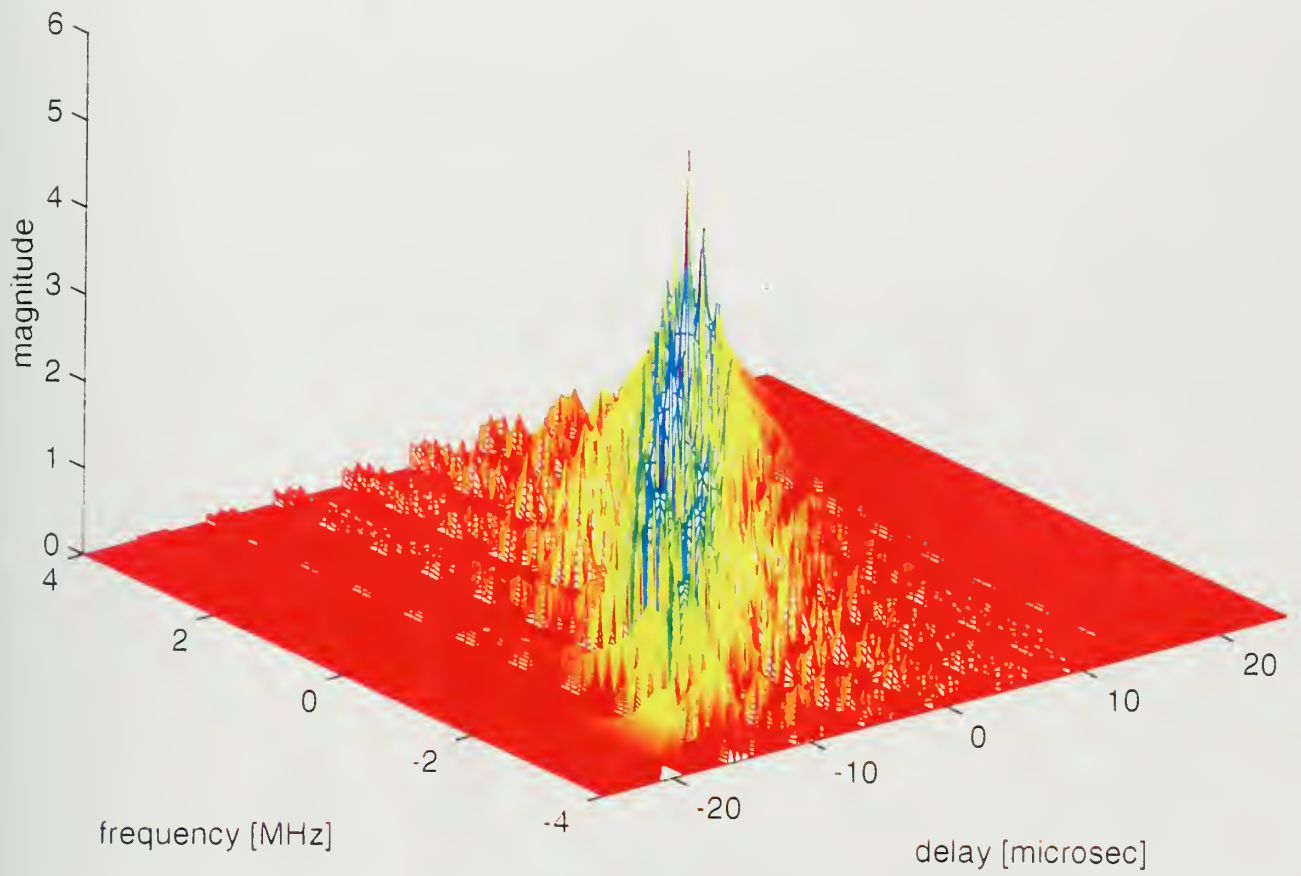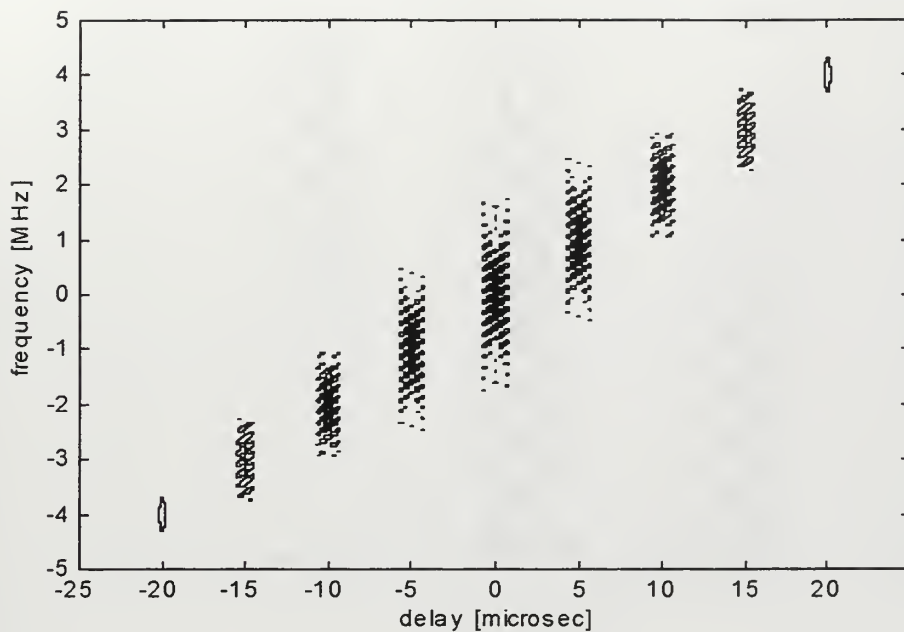Figure 22. Frequency profile of the ambiguity diagram of a step frequency waveform.
(N=5, pulse width =1 microsec, PRI=5 microsec, Δf=1MHz)
(a) Global view.
(b) Magnified view.

54

the delay domain at f_d=0, which portrays only one peak. This suggests that there is no range ambiguity for the waveform if the target doppler is known. Figure 21(b) is a magnification of Figure 21(a) which gives null-to-null width of 0.4 which is the same as computed from the formula $2/(N\Delta f)$. Note that this is also the output of the matched filter in the time domain. The range resolution of this waveform is 0.2 as given by $1/(N\Delta f)$. Figure 22(a) is a cut of the ambiguity surface along the frequency domain at τ=0. Theory suggests that there should be $(2T/t_s)$-1 peaks in the frequency domain, which is matched by the actual value of 9. Figure 22(b) is a detail of the central peak and should have a null-to-null width of $2/(NT)$ which matches with the actual value of 0.08.

2.   Second waveform

For the second case, the waveform has the same parameters as in the previous one except that the number of pulses is increased to 10. This would affect the range resolution $(1/N\Delta f)$ and the doppler resolution $(1/NT)$ which are now 0.1 and 0.02 respectively. However, some other quantities of interest such as the component contours in the frequency axis stay the same. The results can be observed in Figures 23 through 26. Figure 23(a) gives the global view of the contour plot of the ambiguity diagram for this waveform. Figures 23(b), 24(a) and 24(b) are successively increasing magnifications of the contour plot. Figure 24(b) is a detailed plot of the central peak giving a range resolution and frequency resolution of 0.1 and 0.02, respectively. This can be confirmed in Figures 25(b) and 26(b) which are magnified views of the time and frequency profiles, respectively.

Figure 23.   Contour plots of the ambiguity diagram of a step frequency waveform.
(N=10, pulse width=1 microsec, PRI=5 microsec, Δf=1 MHz)
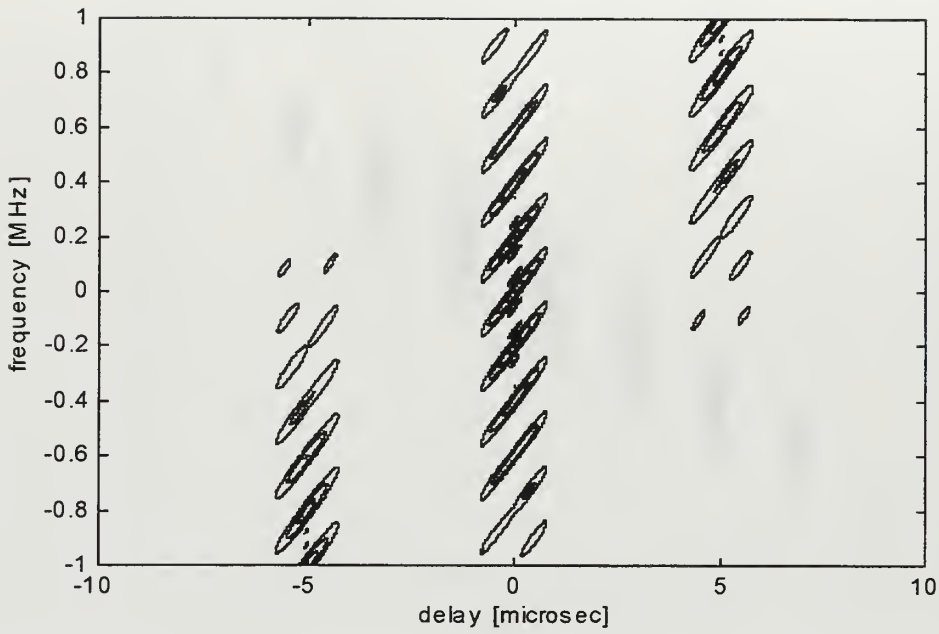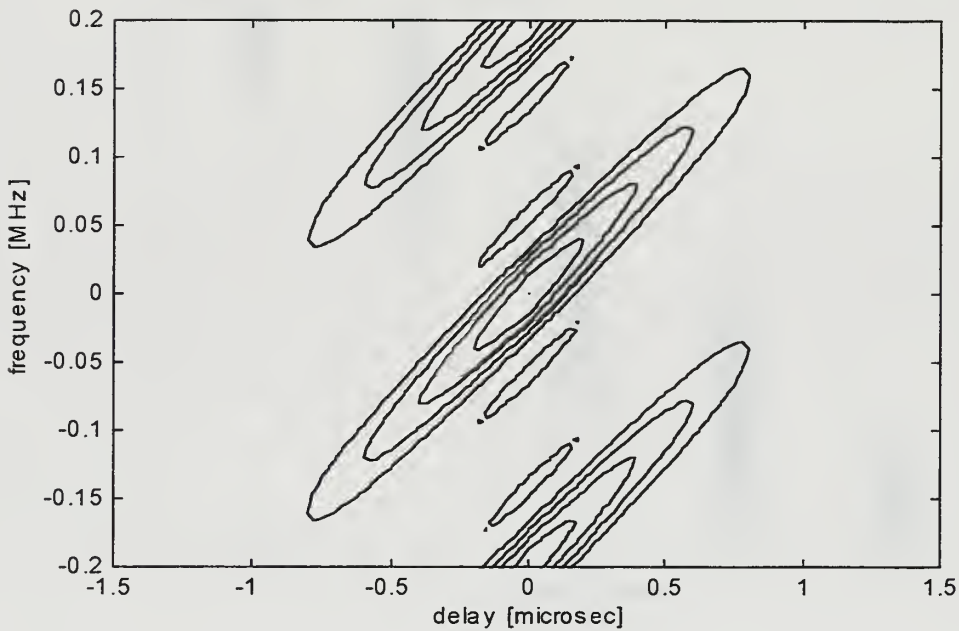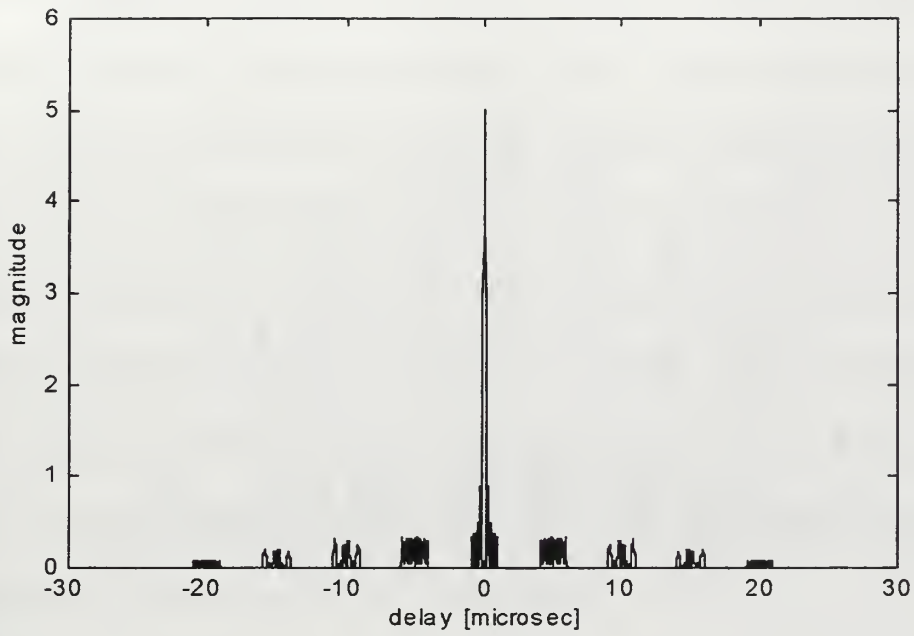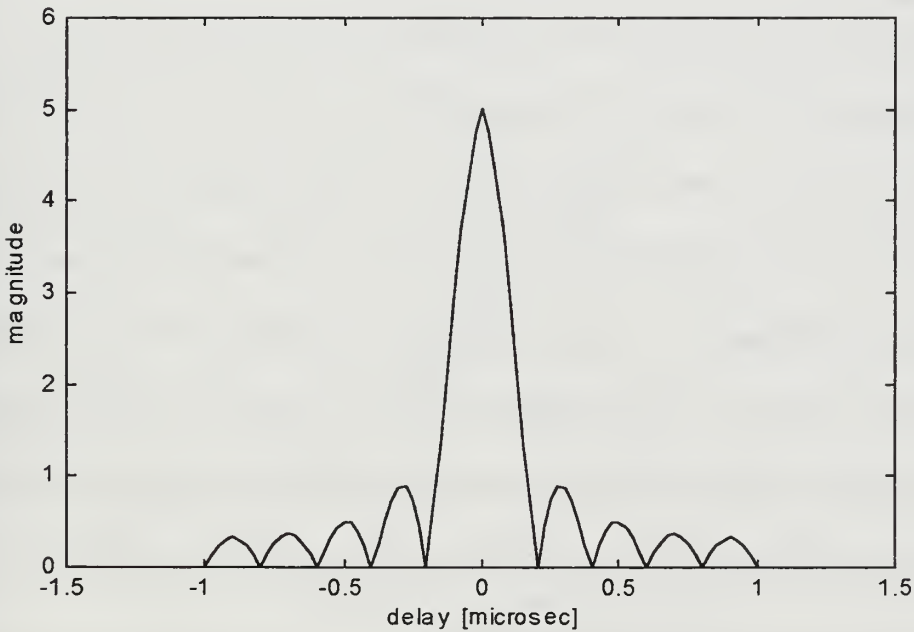(a) Global view.
(b) Magnified view.

(a)

(b)

Figure 24. Contour plots of the ambiguity diagram of a step frequency waveform.
(N=10, pulse width=1 microsec, PRI=5 microsec, Δf=1 MHz)
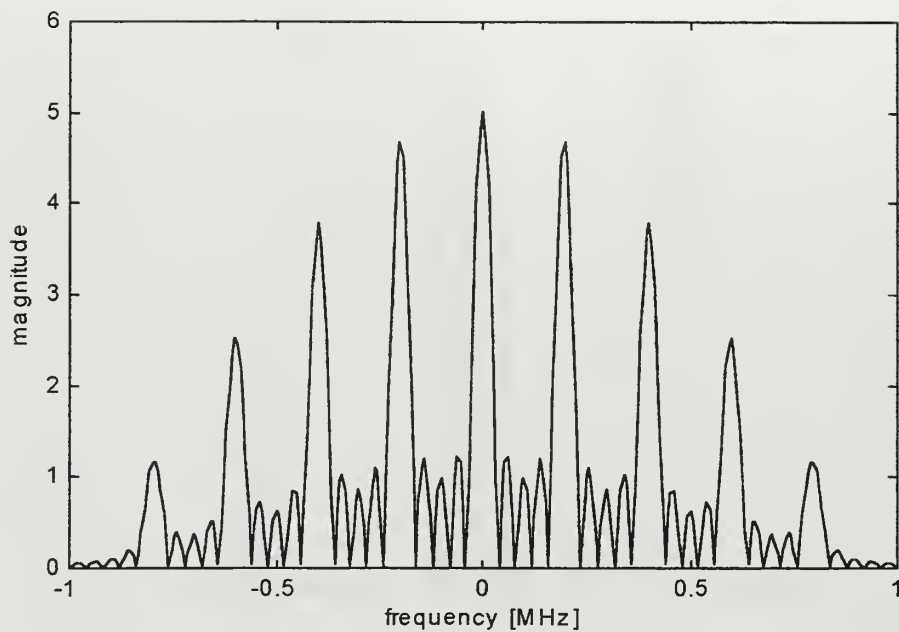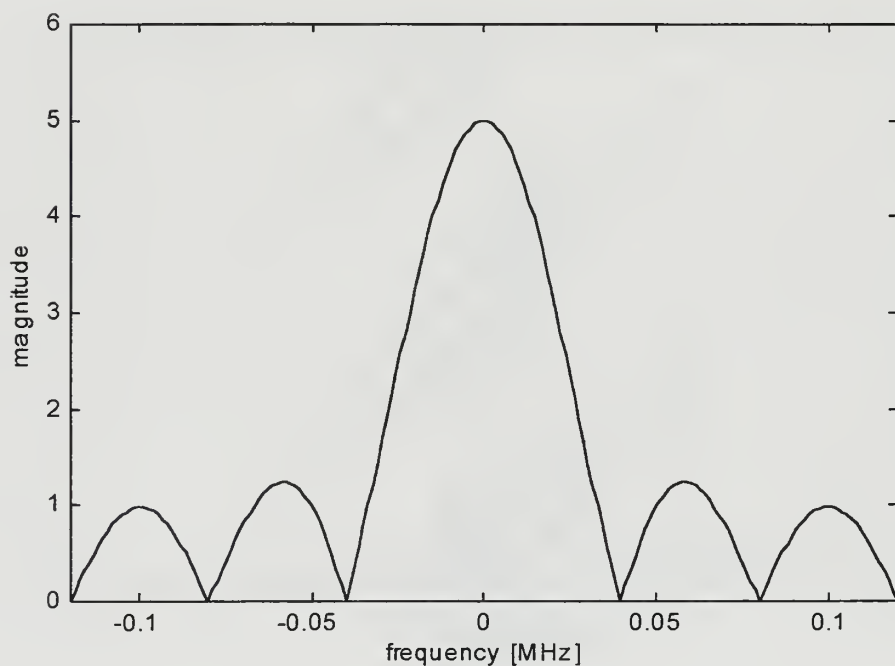(a) Magnified view.
(b) Magnified view of the central peak.

Figure 25. Time profiles (cut at zero frequency) of the ambiguity diagram of a step frequency waveform. (N=10, pulse width=1 microsec, PRI=5 microsec, Δf=1MHz)

                (a) Global view.
                (b) Magnified view.

Figure 26. Frequency profiles of the ambiguity diagram of a step frequency waveform.
(N=10, pulse width =1 microsec, PRI=5 microsec, Δf=1MHz)
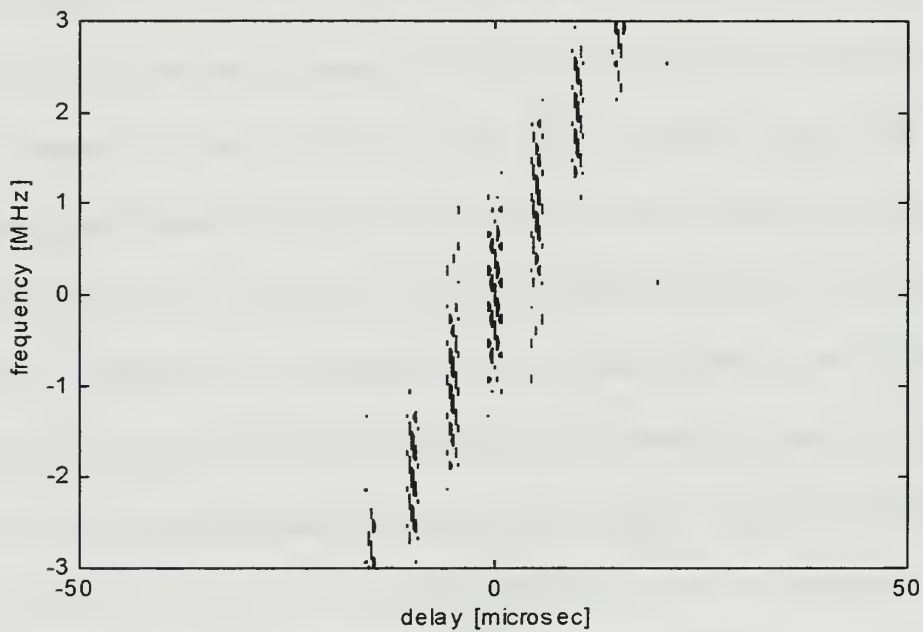(a) Global view.
(b) Magnified view.

59

3.   Third waveform

For this waveform the pulse width is reduced to 0.1 μs and the rest of the parameters are the same as in the previous case. The results can be observed in Figures 27 through 32. Figure 29 represents the central peak of the ambiguity diagram of this step frequency waveform which is similar to the one in Figure A.5.

Now that all the theoretical dimensions previously defined were verified, they can be used to calculate the dimensions of any particular case of interest. This will be done for the fourth and last case.

4.   Fourth waveform

Using the results from Section F, which have been confirmed for the waveforms discussed so far, ambiguity diagram figures were sketched for a waveform with 500 pulses. The amount of computations required to generate the ambiguity surface by computer is enormous. The 3D ambiguity diagram of this waveform is several magnitudes more complex than 3D pictures of midtown Manhattan. One can realize the problem of resolution of this figure and its printing on a normal size paper or even in a much larger size of paper.

A contour plot of the ambiguity diagram is sketched in Figure 33. Each short slant line is a spike. In doppler dimension the spikes are PRF (200 KHz) apart and spread over $2/t_s$ (20 MHz). In delay dimension (at $f_d=0$) there are about ten significant spikes (in reality there are more but others will be small in magnitude). This means that the IF filter will pass ten frequency lines, which implies that the return from ten different ranges due to separate pulses may arrive at the same time. Thus, one may say that the target will be ambiguous in range and that it can lie in any of the ten range zones. Apart from the fact that the target range ambiguity
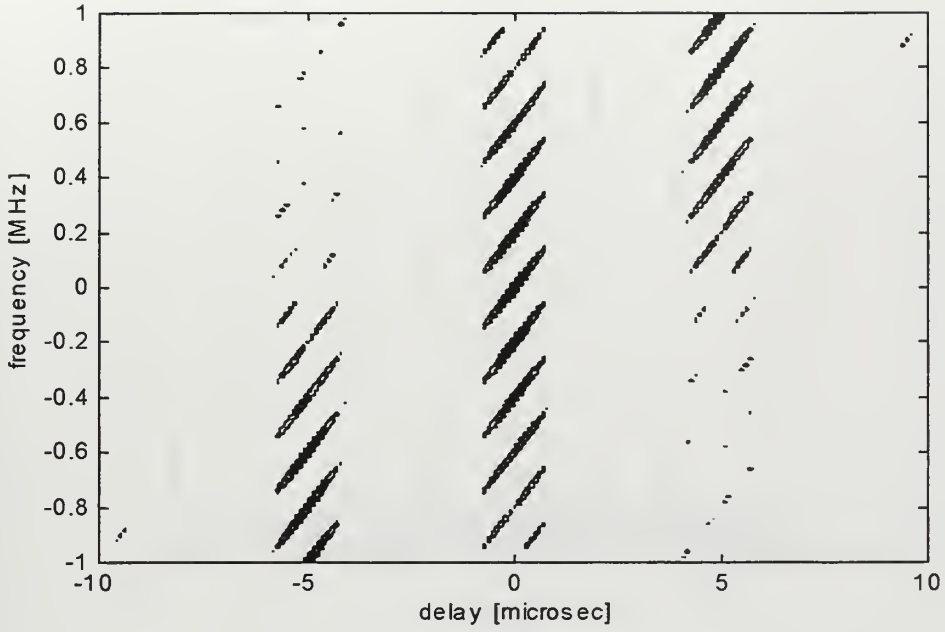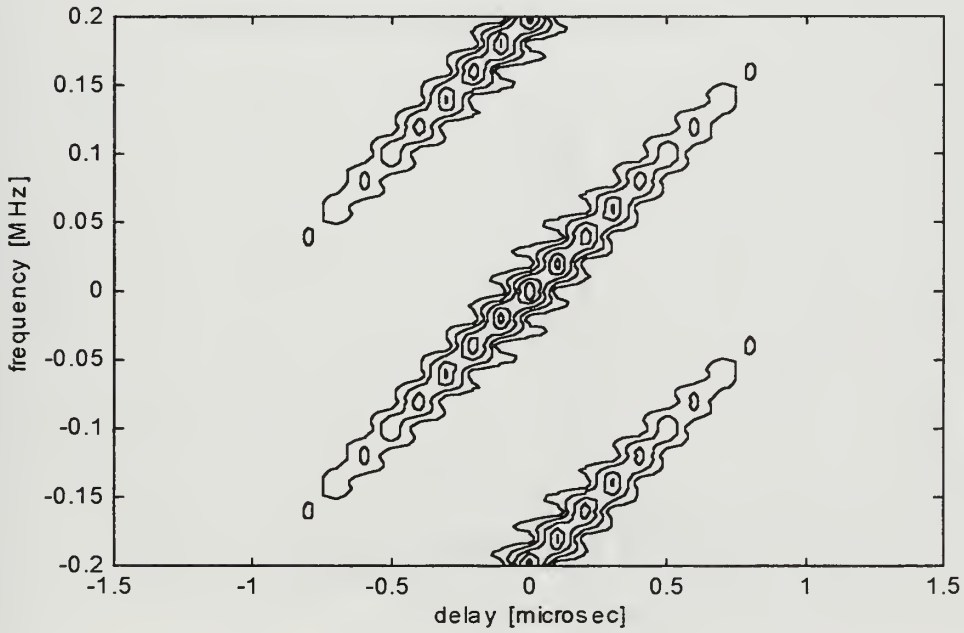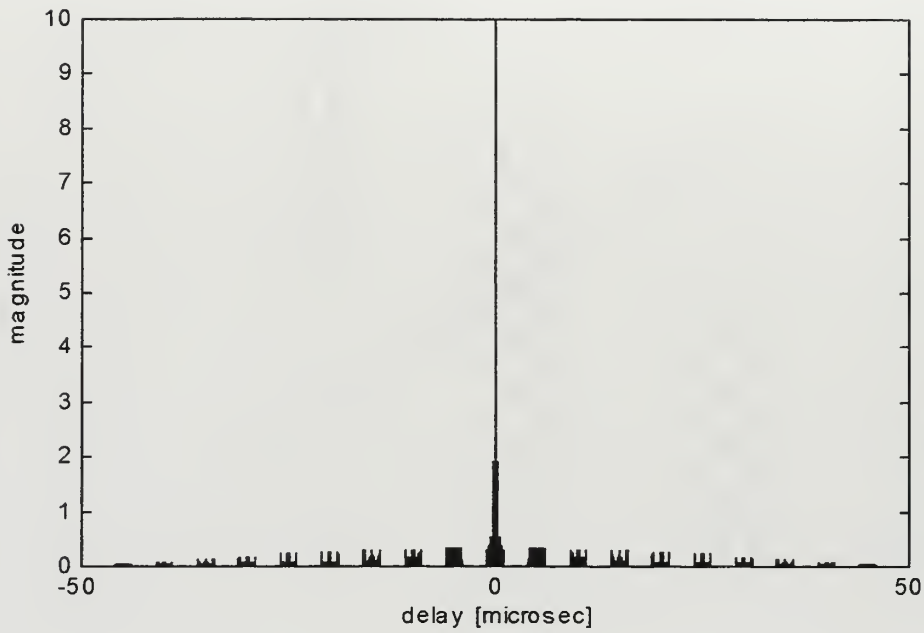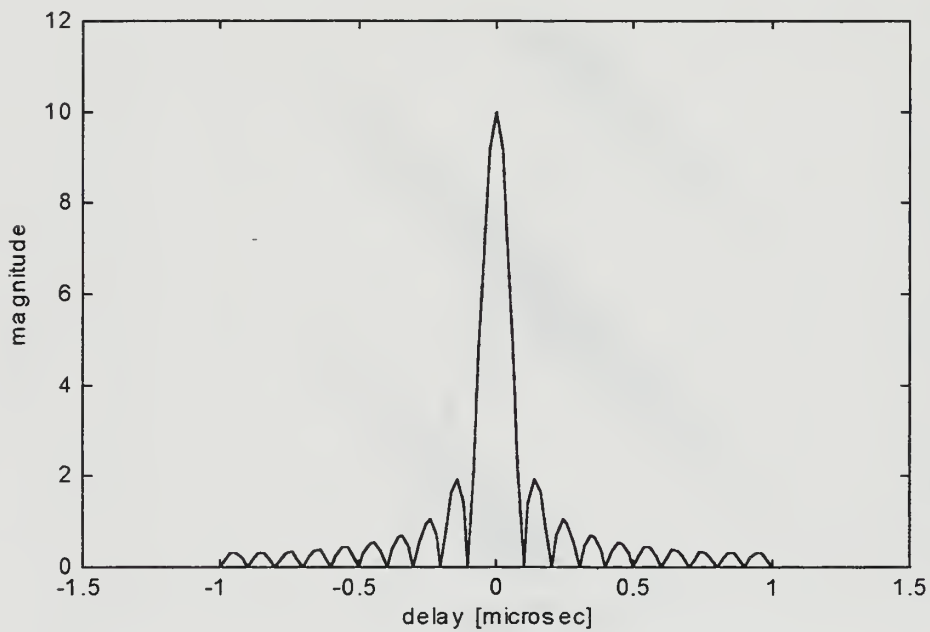
Figure 27. Contour plot of the ambiguity diagram of a step frequency waveform.
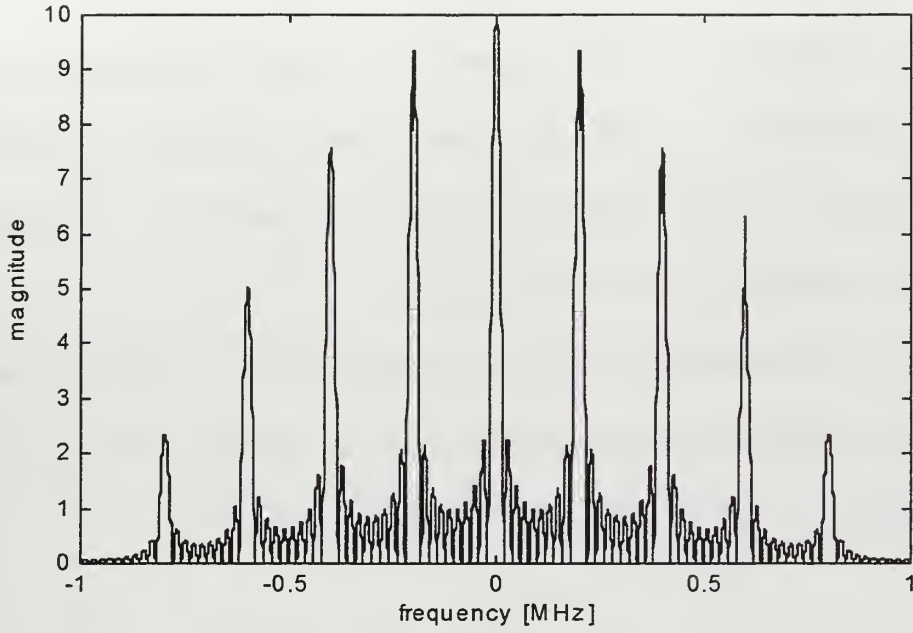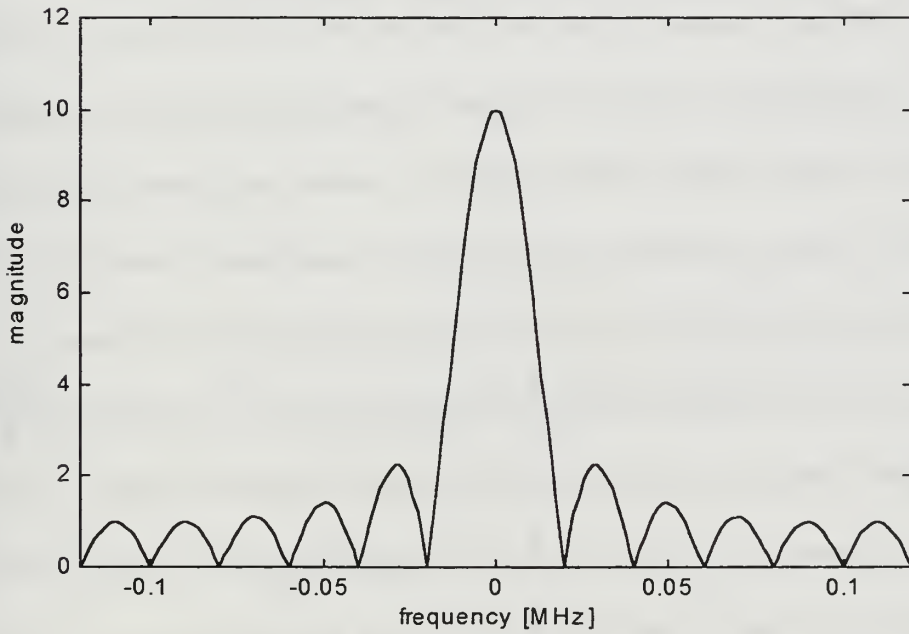(N=10, pulse width=0.1 microsec, PRI=5 microsec, Δf=1 MHz)

Figure 28. Time profile (cut at zero frequency) of the ambiguity diagram of a step
frequency waveform. (N=10, pulse width=0.1 microsec, PRI=5 microsec
Δf=1 MHz)
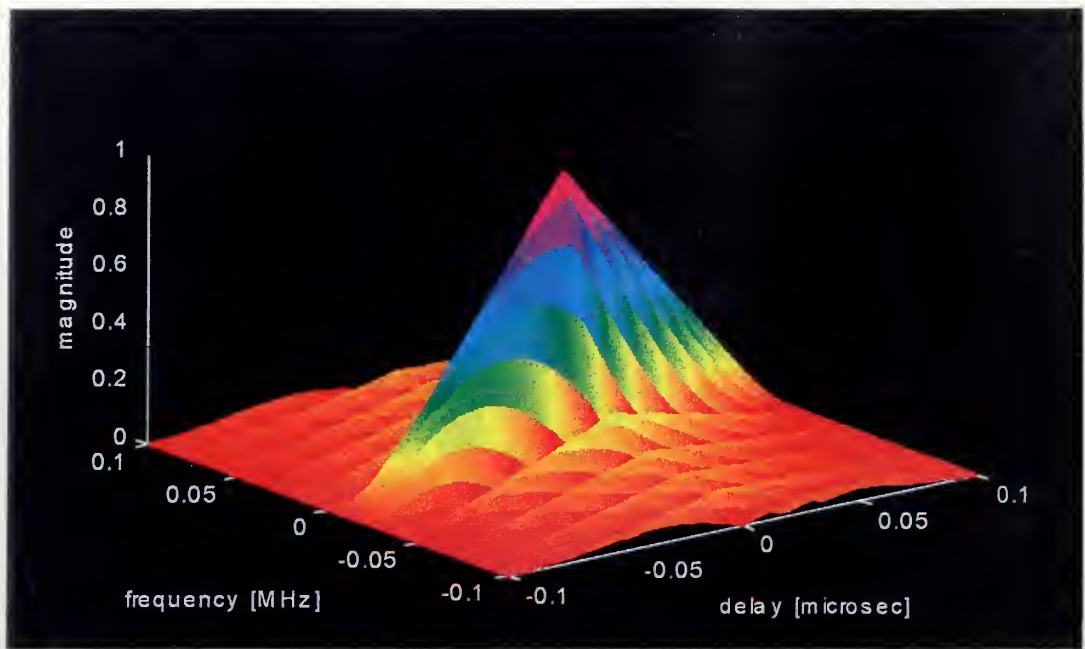
Figure 29. 3D plot of the central peak of the ambiguity diagram of a step frequency waveform. (N=10, pulse width=0.1 microsec, PRI=5 microsec,Δf=1 MHz)
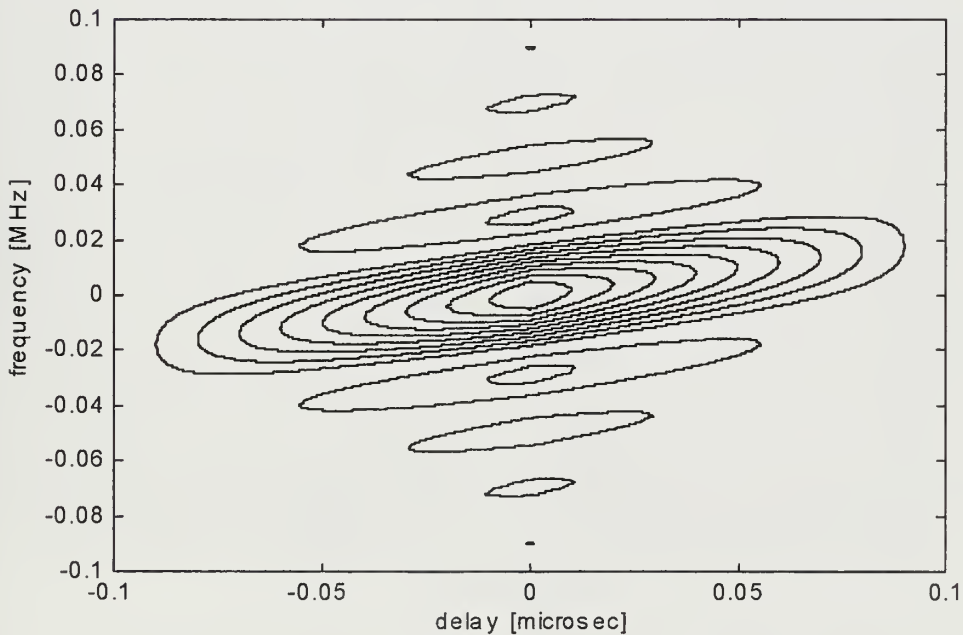
Figure 30. Contour plot of the central peak of the ambiguity diagram of a step frequency waveform. (N=10, pulse width=0.1 microsec, PRI=5 microsec, Δf=1 MHz)
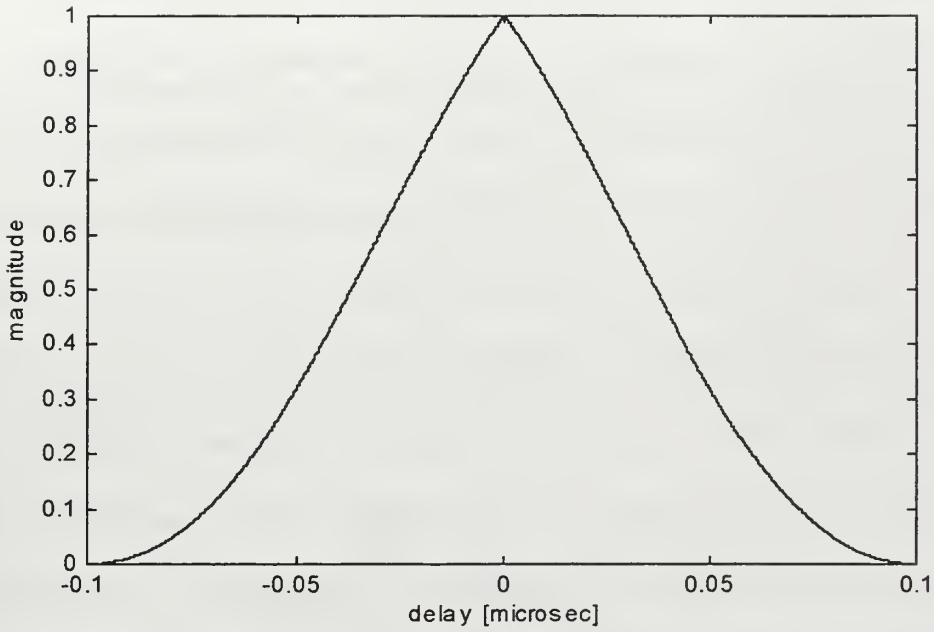
Figure 31. Time profile (cut at zero delay) of the central peak of the step frequency waveform. (N=10, pulse width = 0.1 microsec, PRI = 5 microsec, Δf=1MHz)
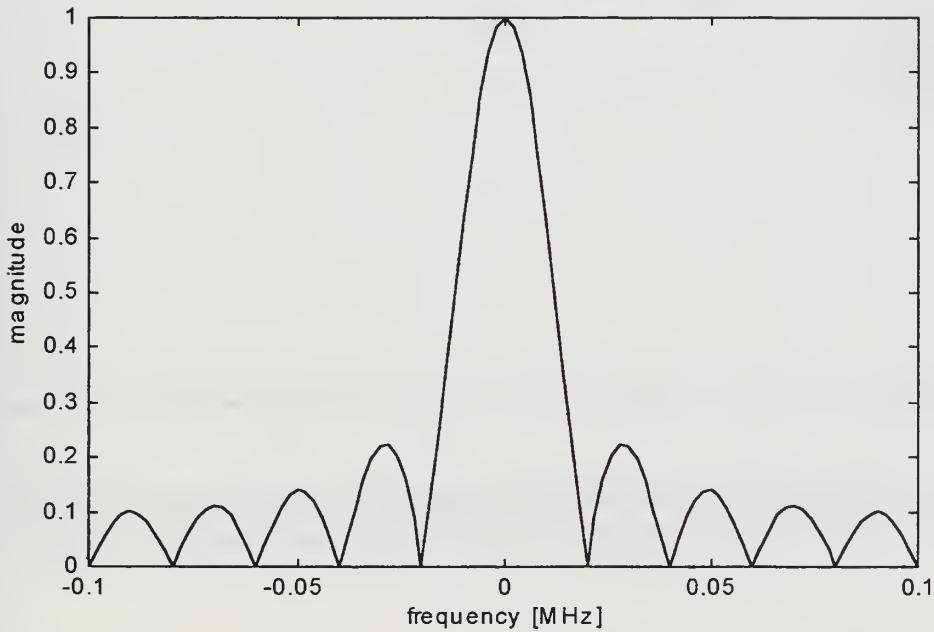
Figure 32. Frequency profile (cut at zero delay) of the central peak of a step frequency waveform. (N=10, pulse width=0.1 microsec, PRI=5 microsec, Δf=1 MHz)
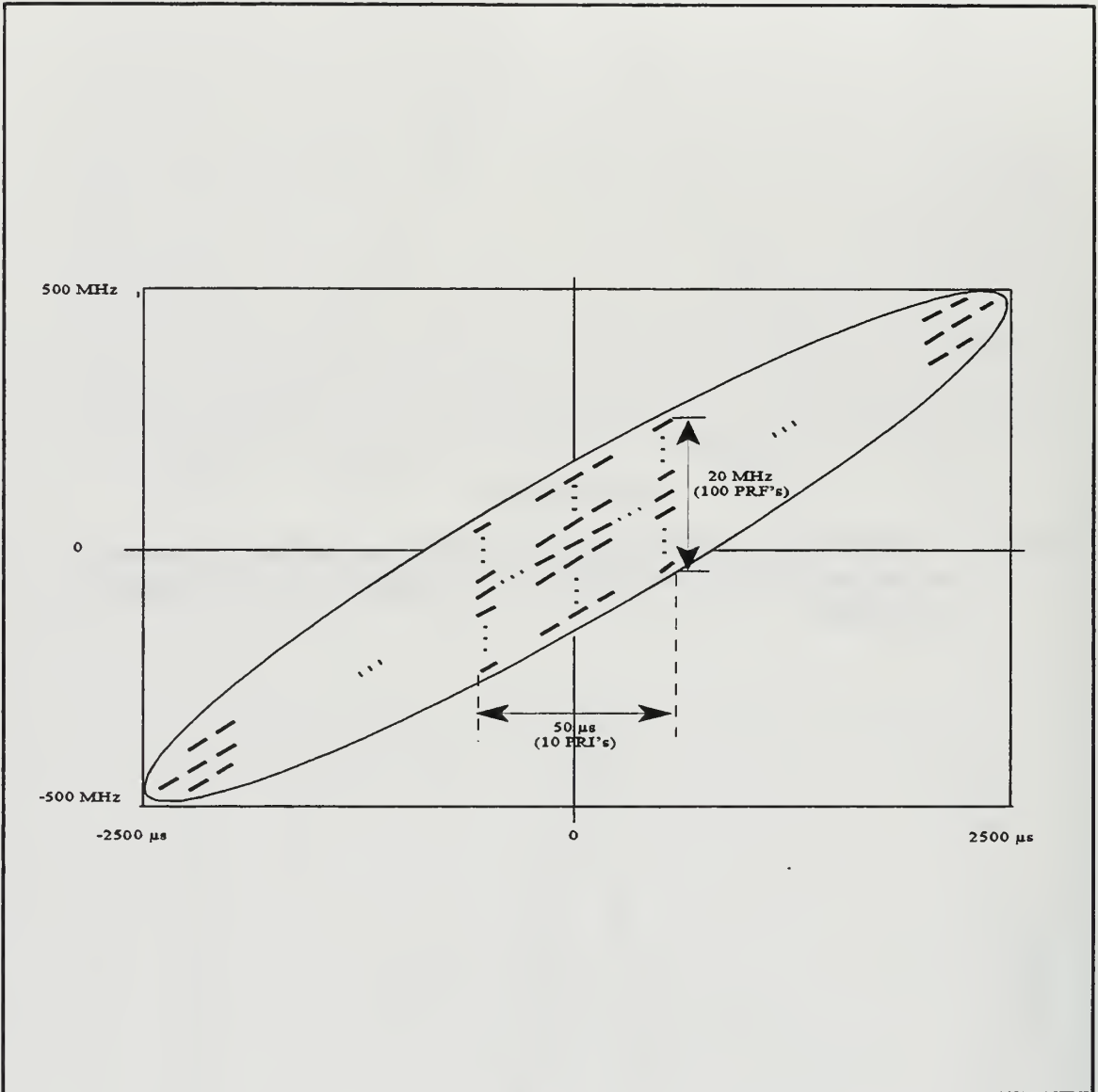
Figure 33. Contour plot of the ambiguity diagram of a step frequency waveform. (N=500, pulse width=0.1 microsec, PRI=5 microsec, Δf=1 MHz)

needs to be resolved it will also compete against clutter from ten different range zones.

If the waveform parameters are picked up judiciously, the doppler from a target moving at the highest expected velocity may be kept unambiguous. In such cases, spikes along the doppler dimension may be ignored, otherwise they have to be considered for clutter calculations. Figures 34 and 35 represent cuts along the delay and frequency dimensions indicating the potential range and doppler ambiguities, respectively. Figure 36 gives the detail of the central peak (note that other peaks or spikes are of similar shape but may be of different magnitude and located at different places in range-doppler map). At f_d =0 the peak is 4 ns wide (null-to-null) in delay dimension. Similarly, the width of the peak in frequency dimension (at τ=0) is given by 2/NT which comes out to be 800 Hz.
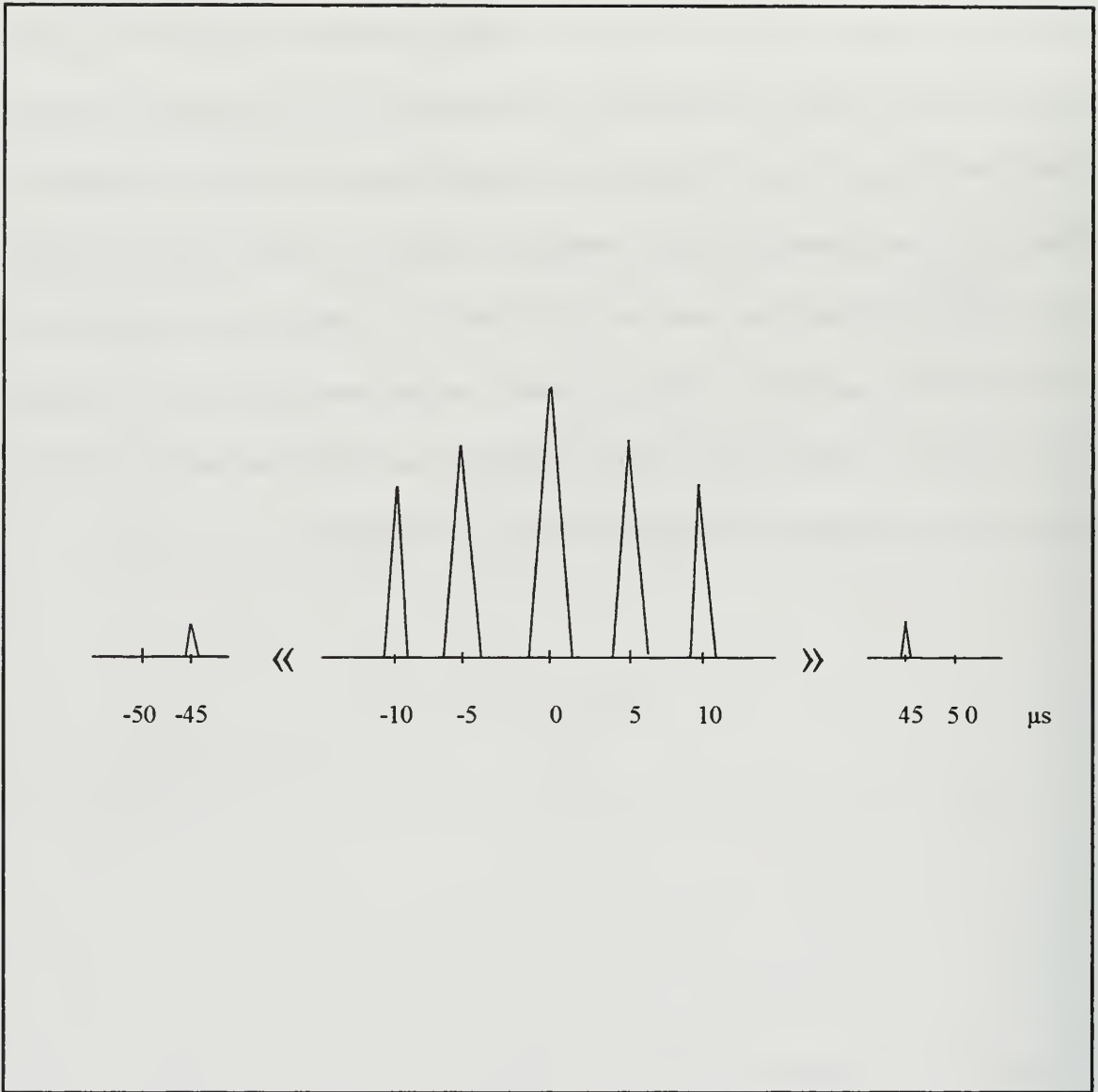
Figure 34. Time profile (cut at zero frequency) of the ambiguity diagram of a step frequency waveform. (N=500, pulse width=0.1 microsec, PRI=5 microsec, Δf=1 MHz)
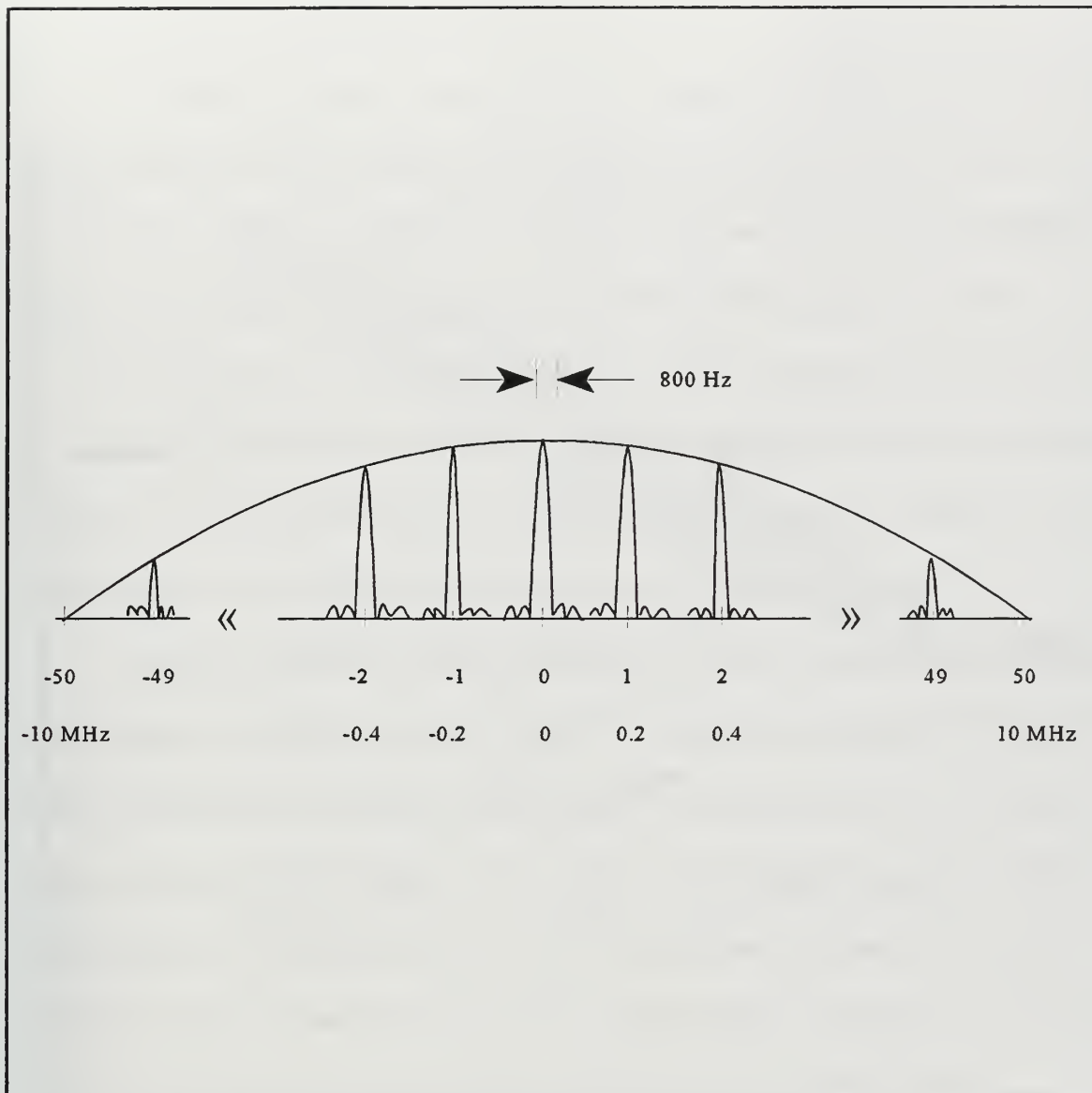
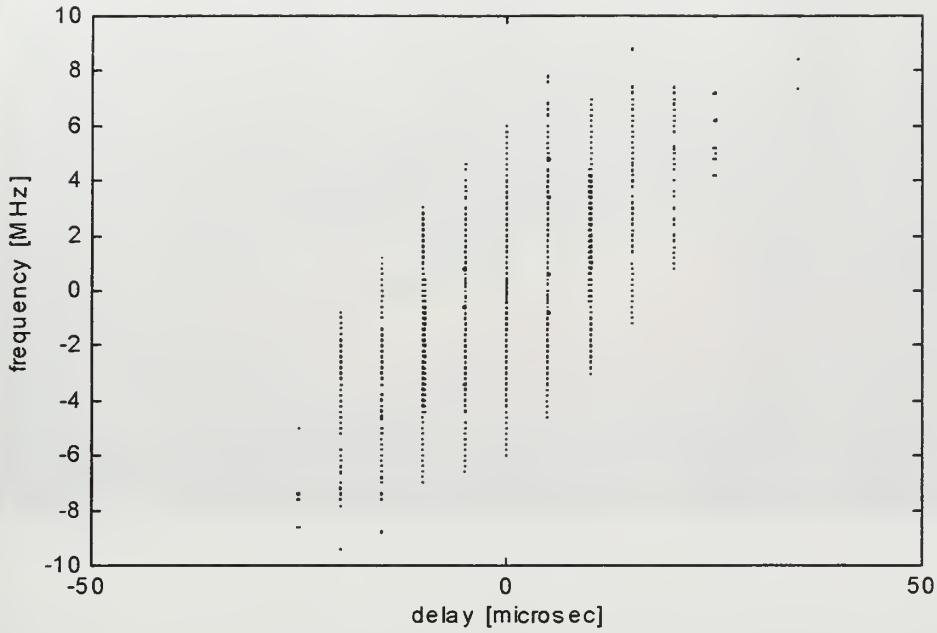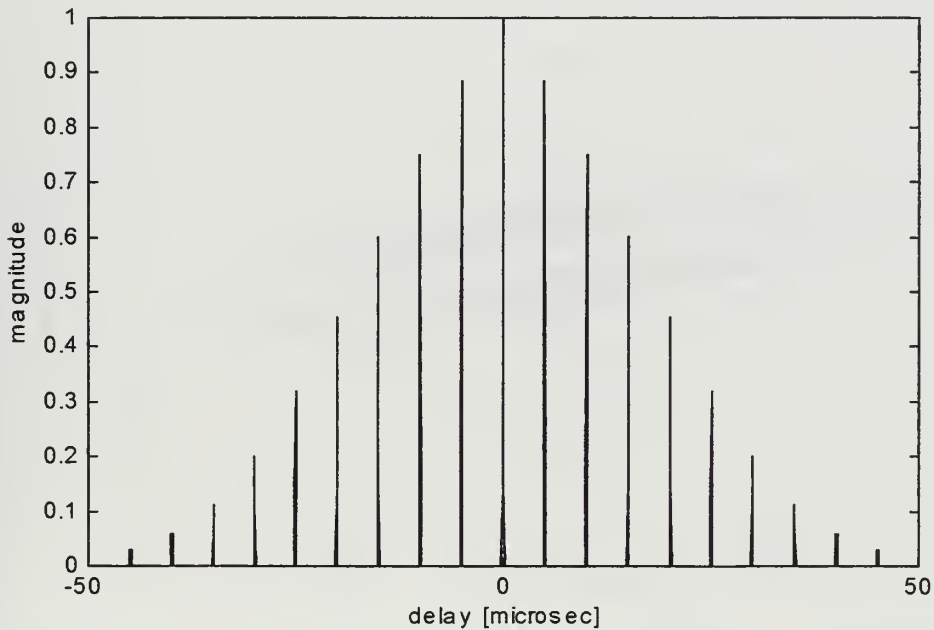Figure 35. Frequency profile (cut at zero delay) of the ambiguity diagram of a step frequency waveform. (N=500, pulse width=0.1 microsec, PRI=5 microsec, Δf=1 MHz)
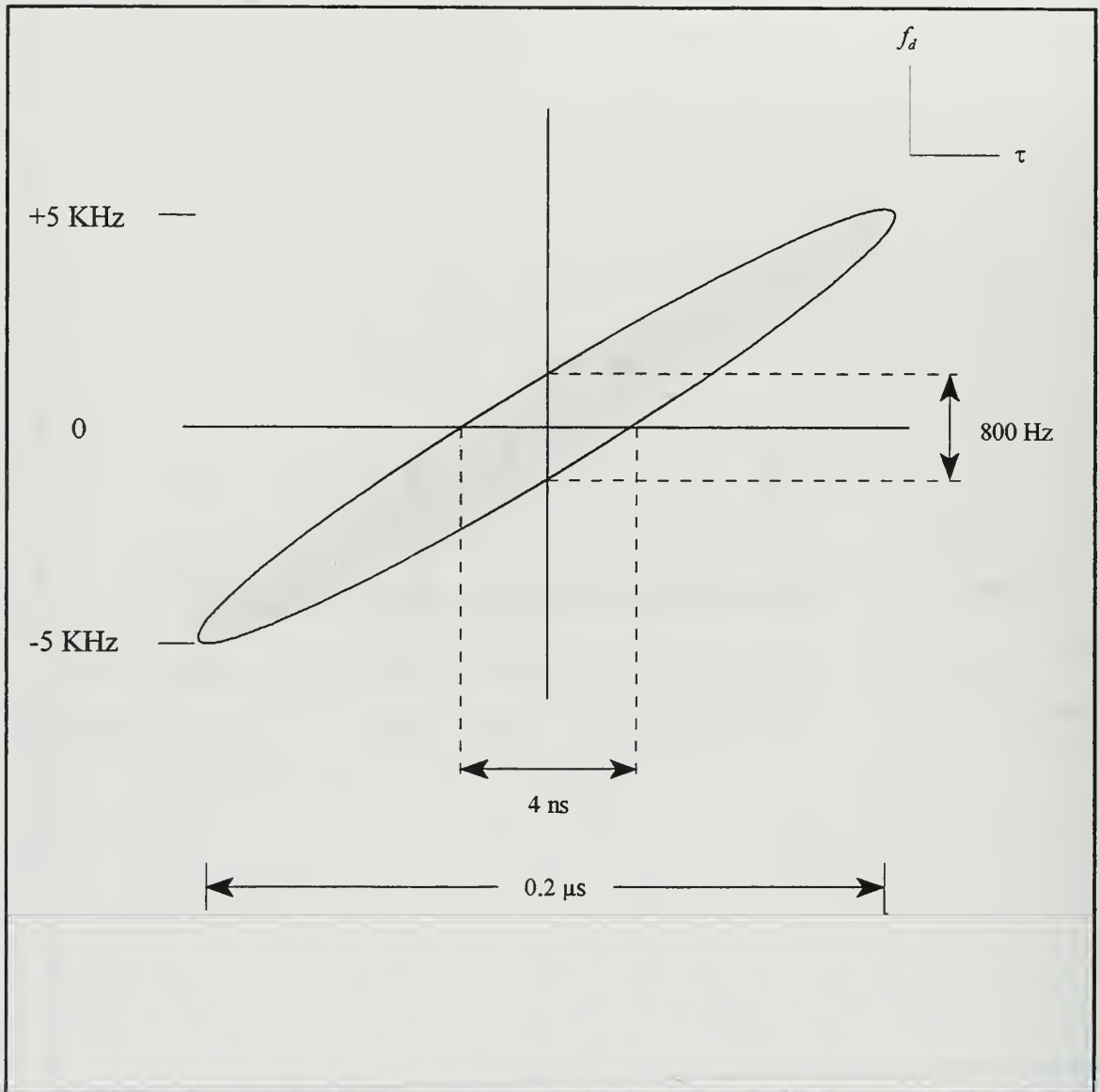
Figure 36. Dimensions of the central peak for the case N=500, pulse width = 0.1 μs, PRI = 5 μs, Δf = 1 MHz. (Values indicated are null-to-null; generally 3dB values are given which are a little less than half of the indicated.)

V. CONCLUSIONS

This thesis investigates the use of the step frequency waveform, its design and analysis using the ambiguity function. The step frequency waveform achieves a high range resolution by coherently processing the returns from N transmitted pulses, each with a different carrier frequency, monotonically increased from pulse to pulse. This waveform has two main advantages over the conventional high resolution waveforms. First, the narrow instantaneous bandwidth does not require a high A/D sampling rate which can be a major limitation in the system design and secondly, the step frequency waveform can be implemented on existing radar equipment using a step frequency synthesizer.

A design procedure for detection of small targets with a surface (land or sea) based step frequency radar which employs a high PRF waveform was developed. The proposed method determines the waveform parameters for given radar specifications. Two different implementations of this method were presented: the graphical and the computer implementation. The graphical implementation is a simple and quick way of calculating the minimum design parameters. The computer implementation considers the parameter constraints that are present when designing a waveform and associated equipment.

The ambiguity function, an important tool for the analysis of any waveform, was defined along with its properties. A practical step frequency waveform may include hundreds of pulses. It is difficult to compute the ambiguity function of a waveform with a large number of pulses. Waveforms with parameters close to the waveform of practical interest but easier to compute were investigated, in order to bring out the key characteristics of the waveform of interest. The theoretical dimensions of the step frequency waveform were defined and

verified with a few different cases. Once this was done, any particular case of interest could be investigated. The ambiguity diagram of one step frequency waveform of interest was sketched. The ambiguity function of the step frequency waveform contains elements of the ambiguity function of a single LFM pulse and train of constant frequency pulses. The 3D plot of the ambiguity function of a step frequency waveform is spiky like the one of a constant frequency pulse train and is tilted at an angle like LFM. The width of the central spike along the delay axis at zero frequency is $2/(N\Delta f)$ as compared to $2t_s$ for the constant frequency pulse train, therefore allowing to decrease the width of the spike by increasing the product $N\Delta f$. This permits increasing the range resolution without increasing the instantaneous bandwidth. For the constant frequency pulse train, high range resolution can only be achieved if the pulse width is decreased. This will cause the increase of the instantaneous bandwidth and therefore a higher A/D sampling rate. On the frequency axis, the spike width at zero delay is equal to $2/(NT)$ as it also for the constant frequency pulse train case. Therefore, the frequency resolution is not improved with the step frequency waveform.

Further work on the comparative analysis of step frequency waveform should be performed to compare it with conventional high PRF and medium PRF waveforms for detection of small targets. Its use in inverse synthetic aperture radar (ISAR) for target identification should also be investigated.

APPENDIX A

This appendix contains the figures for Chapter IV, Section C - Ambiguity function of a single pulse, which are Figures A.1 through A.4. It also contains the figures for Section D - Ambiguity function of the linear frequency modulated pulse, which are Figures A.5 through A.8.
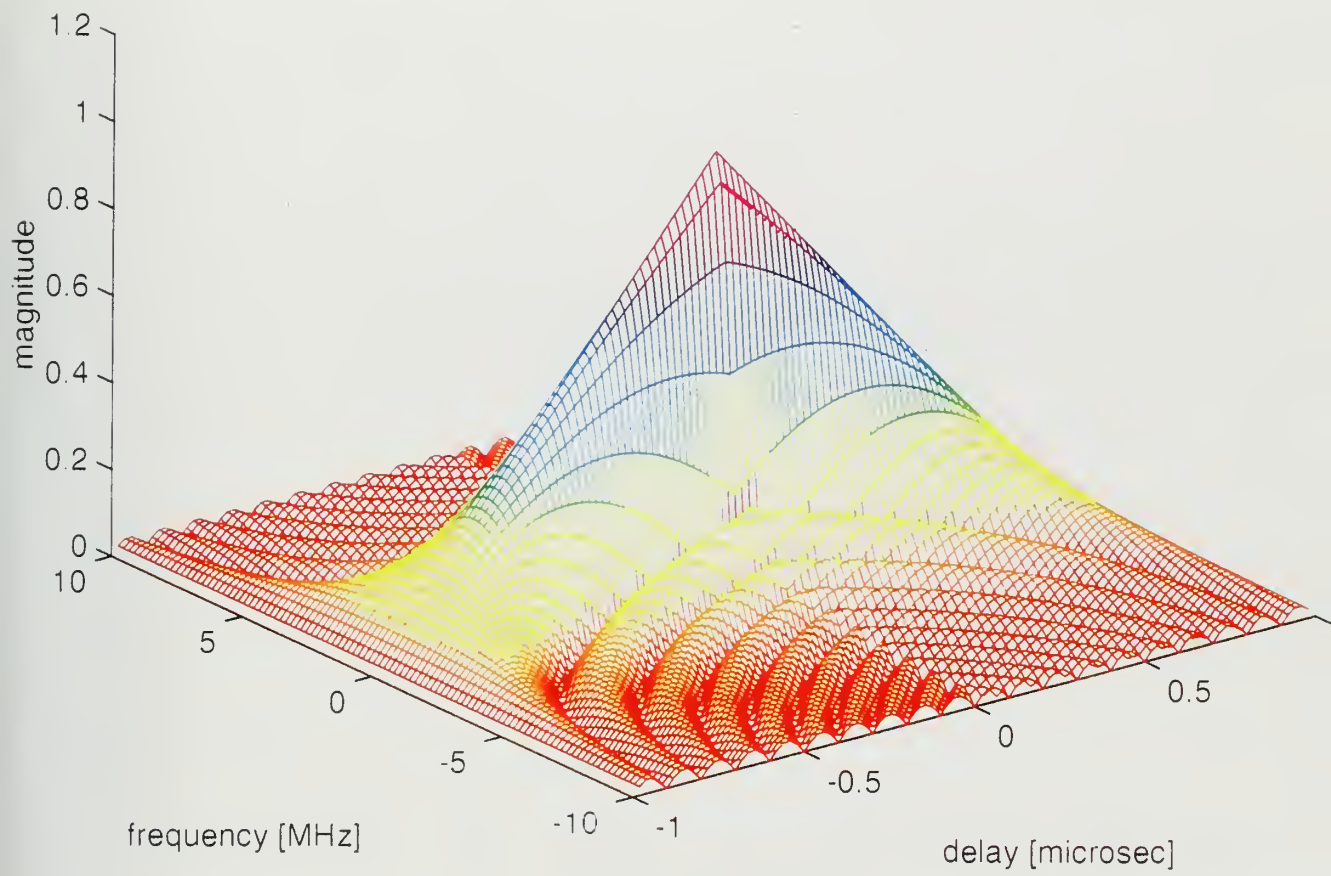
Figure A.1   Ambiguity diagram of a single pulse.

(pulse width=1microsec)

72
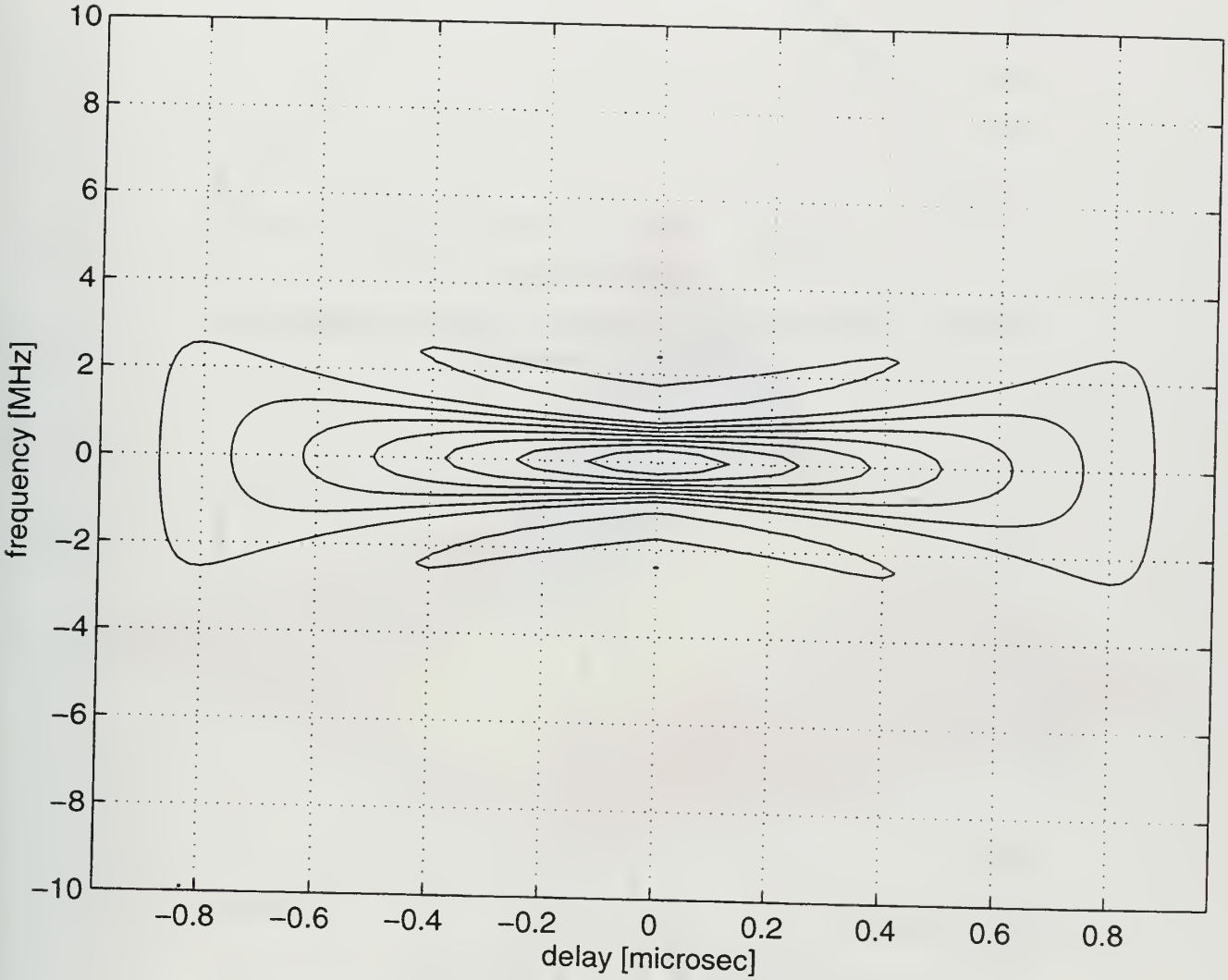
Figure A.2. Contour plot of the ambiguity diagram of a single pulse.

(pulse width=1microsec)

73
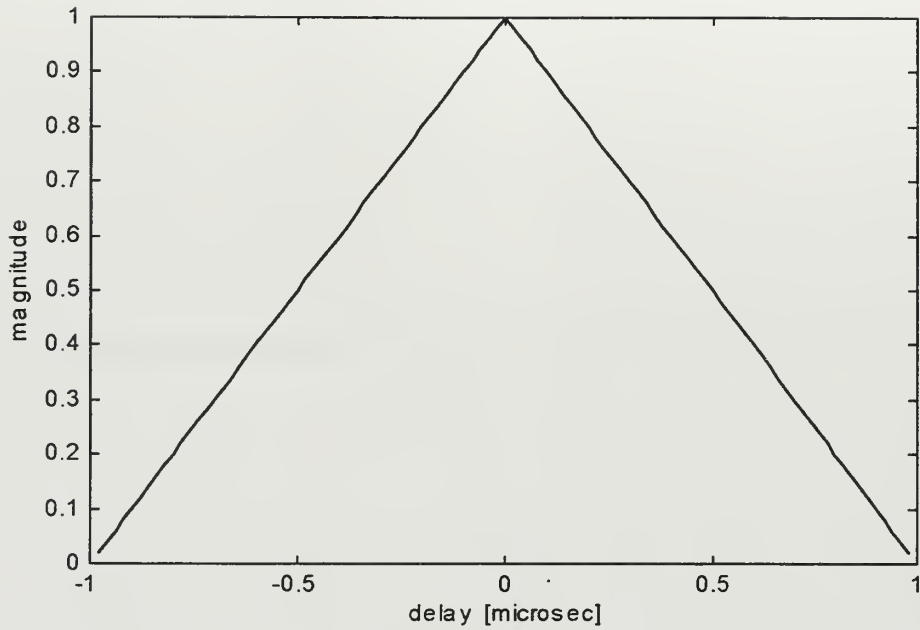
Figure A.3. Time profile of the ambiguity diagram of a single pulse.
(pulse width =1 microsec)
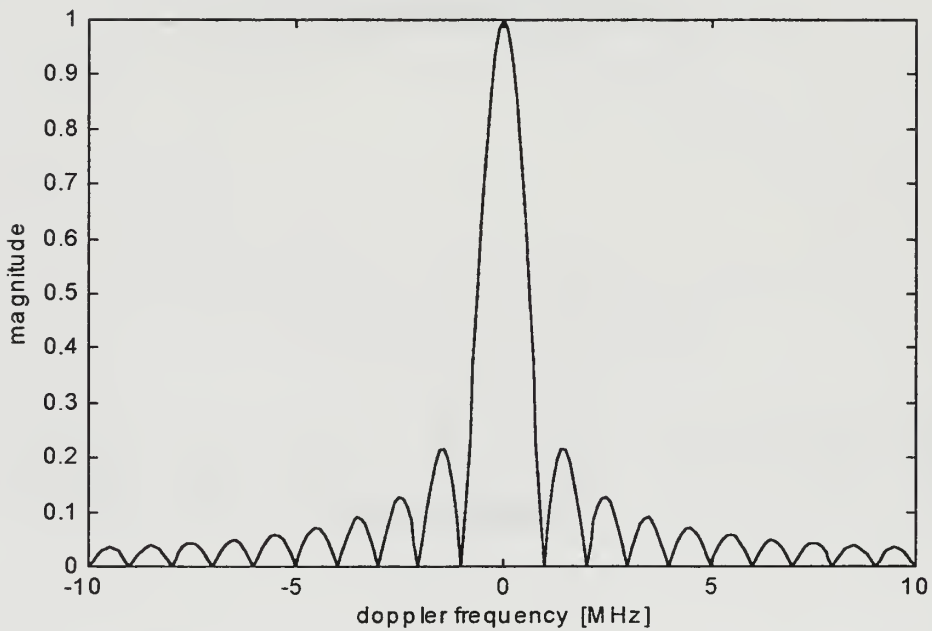
Figure A.4. Frequency profile of the ambiguity diagram of a single pulse.
(pulse width =1 microsec)
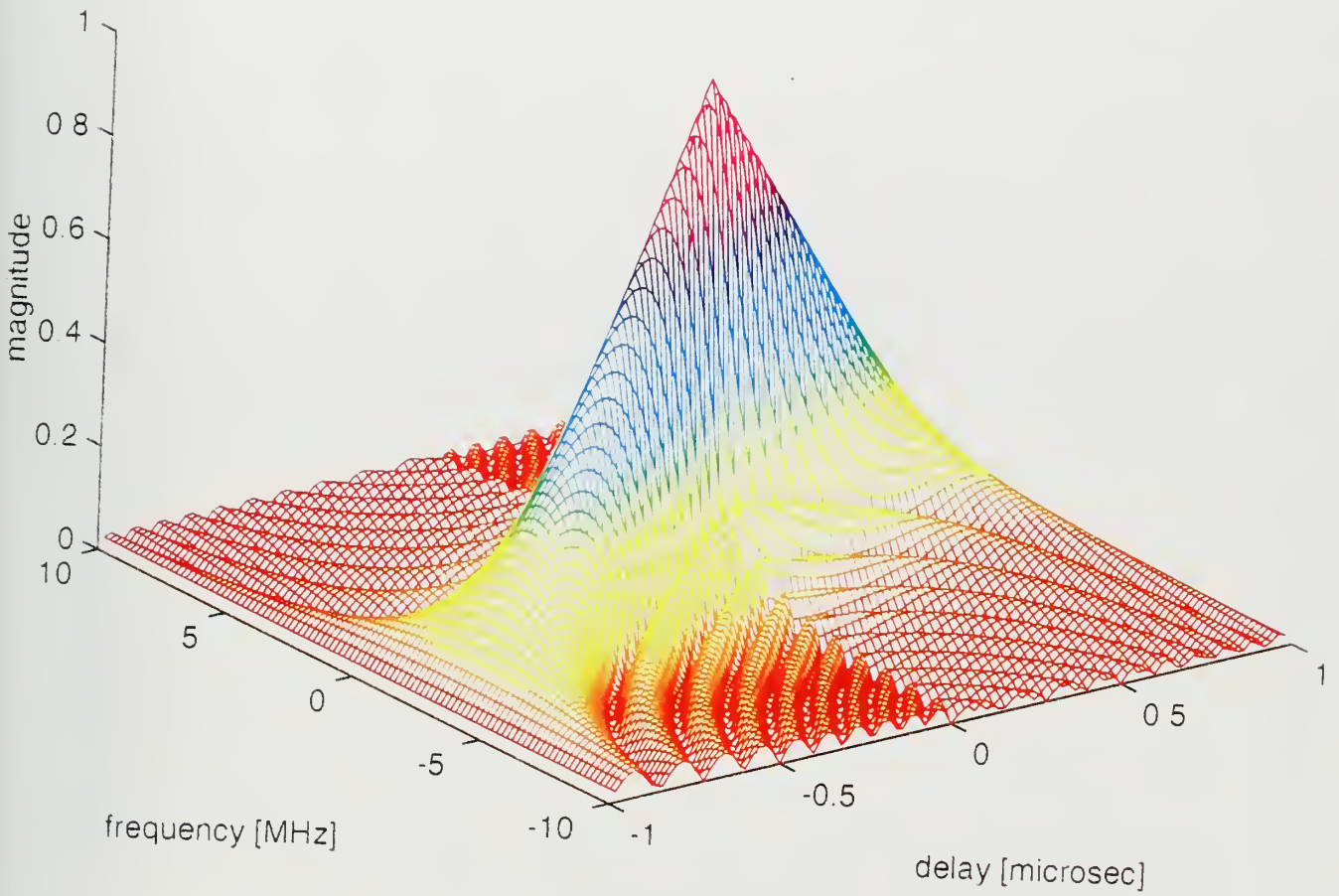
Figure A 5 Ambiguity diagram of a LFM pulse
(pulse width=1 microsec)
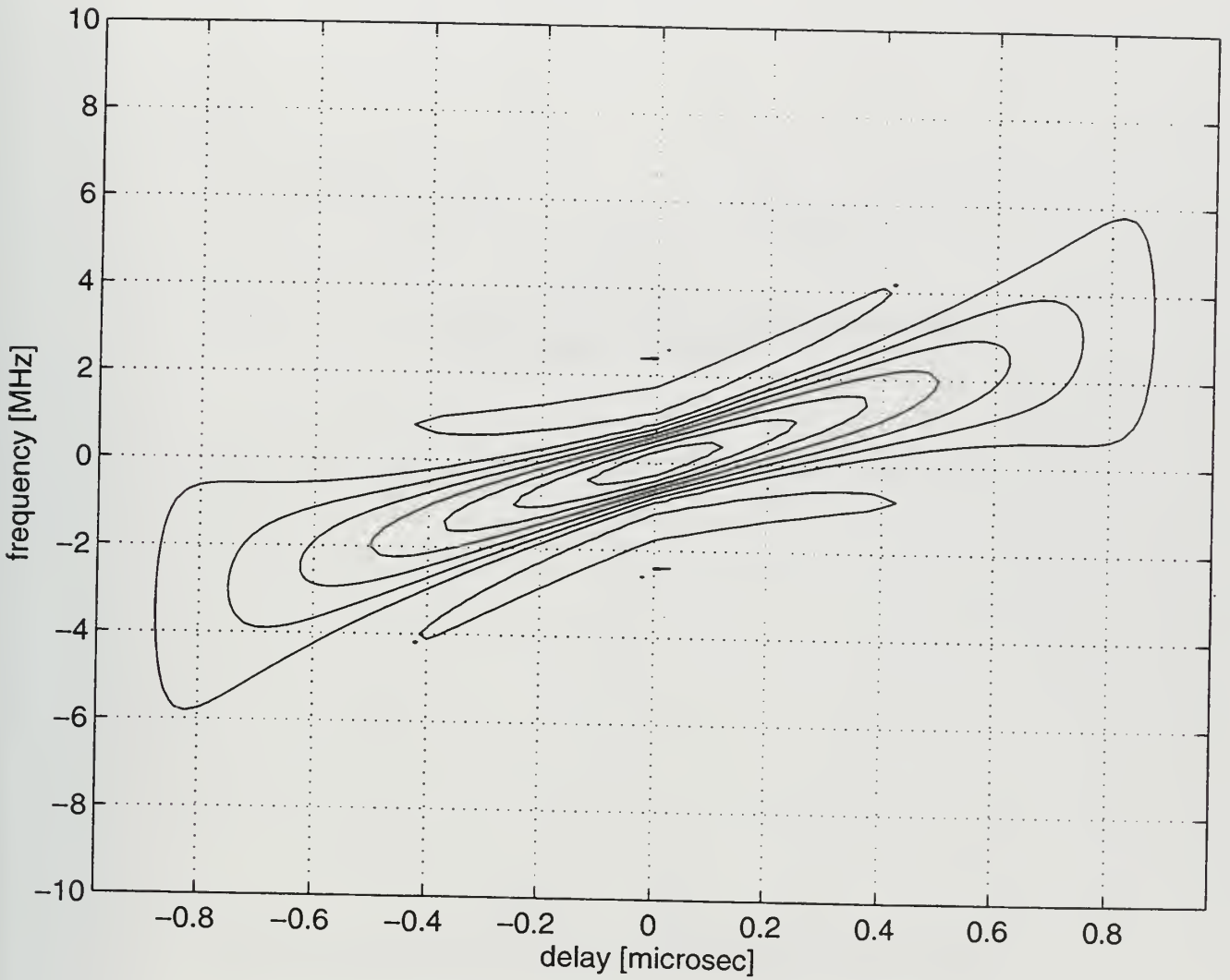
Figure A.6. Contour plot of the ambiguity diagram of a LFM pulse.

(pulse width=1microsec)
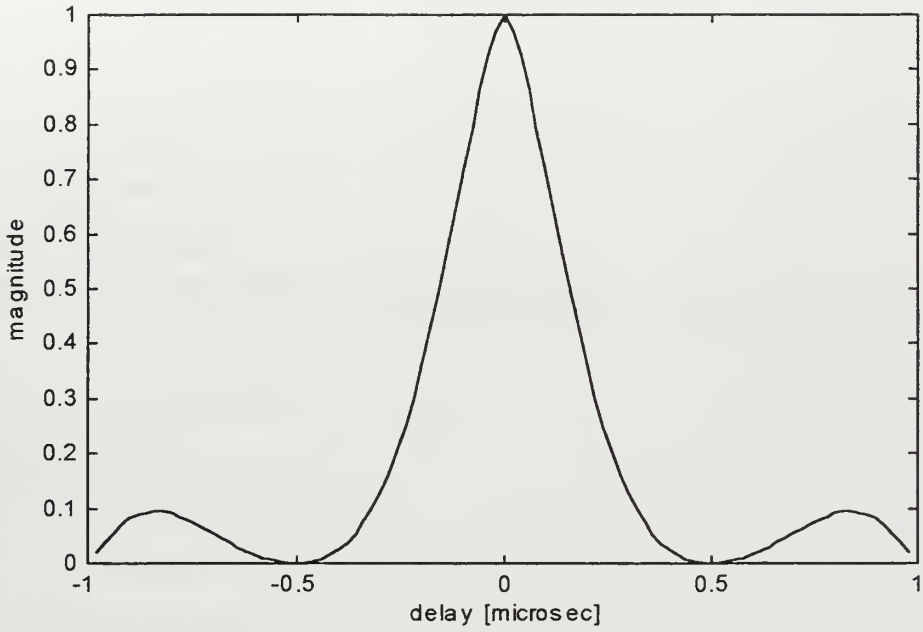
Figure A.7. Time profile of the ambiguity diagram of a LFM pulse.
(pulse width =1 microsec)
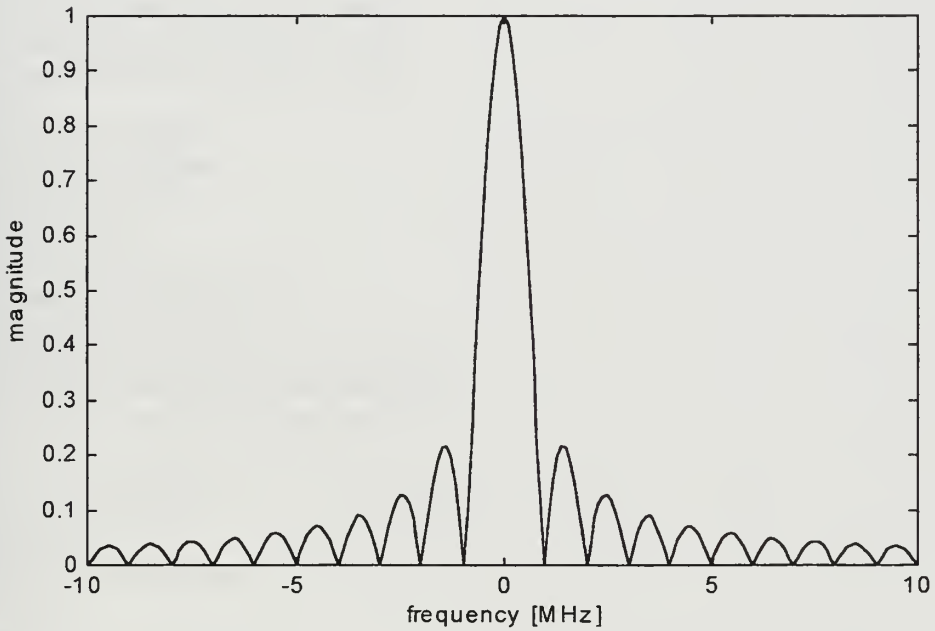
Figure A.8. Frequency profile of the ambiguity diagram of a LFM pulse.
(pulse width =1 microsec)

APPENDIX B.   MATLAB SOURCE CODES

```
% File name: program1.m
% Title: Plot generation
% Date of last revision: 4 Mar 1996
% Written by: Paulo A. Soares
% Comments: This program generates 3 plots for the SFWF design.
%*******************************************************************************

clear
% ------------------- specifications ----------------------
vmin=150;vmax=1000;
f01=3e9;f02=5e9;f03=7e9;f04=10e9;
tot1=5e-3;tot2=10e-3;tot3=15e-3;tot4=20e-3;

% ---------------- computations & plots ------------------
c=3e8;
lambda1=c/f01;lambda2=c/f02;
lambda3=c/f03;lambda4=c/f04;

-% ---------------------- plot #1 -------------------------
dr=0.01:0.01:1;
fr1=(dr.\vmax)+((2/lambda1)*(vmax+vmin));
fr2=(dr.\vmax)+((2/lambda2)*(vmax+vmin));
fr3=(dr.\vmax)+((2/lambda3)*(vmax+vmin));
fr4=(dr.\vmax)+((2/lambda4)*(vmax+vmin));
figure(1)
  plot(dr,fr1/1e3,'w'),hold on
  plot(dr,fr2/1e3,'w'),hold on
  plot(dr,fr3/1e3,'w'),hold on
  plot(dr,fr4/1e3,'w')
  axis([0.01,1,10,110])
  xlabel('Range Resolution (meters)')
  ylabel('Minimum PRF (Khz)')
  text(0.75,27,'fo=3GHz'),text(0.75,42,'fo=5GHz')
  text(0.75,57,'fo=7GHz'),text(0.75,81,'fo=10GHz')
  text(0.2,100,'fo = nominal carrier frequency')

% ------------------------- plot #2 -------------------------
lambda=0.03:0.001:0.129;
k=(dr.\vmax);
fr1=(lambda.\2)*(vmax+vmin)+k;
N11=tot1*fr1;
N21=tot2*fr1;
N31=tot3*fr1;
figure(2)
  plot(fr1/1e3,N11,'w'),hold on
  plot(fr1/1e3,N21,'w'),hold on
  plot(fr1/1e3,N31,'w'),hold on
  axis([20,180,0,3000])
  xlabel('PRF (KHz)')
```

```
  ylabel('N')
  text(140,900,'tot=5ms'),text(140,1700,'tot=10ms')
  text(140,2550,'tot=15ms')
  text(50,2500,'tot = time-on-target')


% ------------------------plot #3------------------------
deltar1=0.3;
deltar2=0.5;
deltar3=1;
N=1:1:2048;
deltaf1=(2*N*deltar1*1e6).\c;
deltaf2=(2*N*deltar2*1e6).\c;
deltaf3=(2*N*deltar3*1e6).\c;
figure(3)
  plot(N,deltaf1,'w'),hold on
  plot(N,deltaf2,'w'),hold on
  plot(N,deltaf3,'w')
  axis([0,2100,0,1])
  xlabel('N')
  ylabel('Frequency Step (MHz)')
  text(1700,0.12,'dr=1m'),text(1700,0.21,'dr=0.5m'),text(1700,0.33,'dr=0.3m')
  text(1200,0.8,'dr = range resolution')
```

```
% Filename: program2.m
% Title: Main program for SFWF design
% Date of last revision: 28 Feb 1996
% Written by: Paulo A. Soares
% Comments: This program computes the exact design  parameters frmin, df, N and tau, and then
%            rounds it in accordance with previously defined criteria.
%*****************************************************************************

clear
c=3e8;Nmax=2048;
vmin=150;vmax=1000;
dr=input(' Enter the desired range resolution in meters : ');
while dr <= 0
  dr=input(' You must enter a positive value. Please try again : ')
end
f0=input(' Enter the nominal carrier frequency in GHz : ');
while f0 <= 0
  f0=input(' You must enter a positive value. Please try again : ')
end
lambda=c/(f0*1e9);
tot=input(' Enter the time-on-target in msec : ');
while tot <= 0
  tot=input(' You must enter a positive value. Please try again : ')
end
 frmin=(((2/lambda)*(vmax+vmin))+(vmax/dr))/1e3;
 fr=ceil(frmin);
while rem(fr,5) ~= 0
 fr=fr+1;
end
Nmin=ceil(tot*fr);
N=Nmin;
if N<=2
 N=2;
end
elseif N==3 | N==4
 N=4;
end
elseif N>4 & N<=9
 N=8;
end
elseif N>9 & N<=17
 N=16;
end
elseif N>17 & N<=34
 N=32;
end
elseif N>34 & N<=68
 N=64;
end
elseif N>68 & N<=136
 N=128;
end
elseif N>136 & N<=272
 N=256;
end
```

81

```
elseif N>272 & N<=544
  N=512;
end
elseif N>544 & N<=1088
  N=1024;
end
elseif N>1088
  N=Nmax;
end
Nround=N;
frround=Nround/tot;
frround=ceil(frround);
while rem(frround,5) ~=0
  frround=frround+1;
end
totround=Nround/frround;
dfmin=c/(2*Nmin*dr*1e6);
df=c/(2*Nround*dr*1e6);
stepsizedf=0.2;
dfround=ceil(df/stepsizedf);
dfround=dfround*stepsizedf;
taumin=(2*vmin)/(lambda*dfmin*frmin);
tau=(2*vmin)/(lambda*dfround*frround);
stepsizetau=10;
tauround=ceil(tau/stepsizetau);
tauround=tauround*stepsizetau;
acdr=(c/(2*Nround*dfround))*1e-6;
stepsizeacdr=0.01;
acdrround=ceil(acdr/stepsizeacdr);
acdrround=acdrround*stepsizeacdr;
fprintf('\n The calculated design parameters are:\n')
fprintf('  (minimum values in brackets)\n\n')
fprintf('  -PRF = %3.2f KHz                (%3.2f KHz)\n',frround,frmin);
fprintf('  -Frequency step = %3.2f MHz          (%3.2f MHz)\n',dfround,dfmin);
fprintf('  -Pulse width = %3.2f nsec          (%3.2f nsec)\n',tauround,taumin);
fprintf('  -Number of pulses = %4.0f          (%4.0f)\n',Nround,Nmin);
fprintf('  -Actual range resolution = %3.2f m\n',acdrround);
fprintf('  -Actual time-on-target = %3.2f msec ',totround);
```

```
% Filename: program3.m
% Title: Ambiguity function of the simple pulse by correlation method
% Date of last revision: 6 Apr 1996
% Written by: Paulo A. Soares
% Comments: This program draws four plots of the ambiguity function for a single pulse.
%****************************************************************************

clear;
tau=1;
nx=50;
ny=201;
t=[0:nx-1]*tau/nx;
dt=t(2)-t(1);
z=[];
fd=linspace(-10/tau,10/tau,ny);
u1=ones(1,nx);
for m=1:ny
 u2=u1.*exp(j*2*pi*fd(m)*t);
 c=xcorr(u2,u1).*dt;
 z=[z;abs(c)];
end
t=[fliplr(-t),t(2:nx)];
figure(1)
 mesh(t,fd,z),grid
 xlabel('delay [microsec]')
 ylabel('frequency [MHz]')
 zlabel('magnitude')
figure(2)
 contour(t,fd,z,7),grid
 xlabel('delay [microsec]')
 ylabel('frequency [MHz]')
figure(3)
 plot(t,z((ny+1)/2,:),'w')
 xlabel('delay [microsec]')
 ylabel('magnitude')
figure(4)
 plot(fd,z(:,nx),'w')
 xlabel('frequency [MHz]')
 ylabel('magnitude')
```

```
% Filename: program4.m
% Title: Ambiguity function of the LFM pulse by correlation method
% Date of last revision: 6 Apr 1996
% Written by: Paulo A. Soares
% Comments: This program draws four plots of the ambiguity function for a LFM pulse.
%***********************************************************************************

clear;
tau=1;
mu=4;
nx=50;
ny=201;
t=[0:nx-1]*tau/nx;
dt=t(2)-t(1);
z=[];
fd=linspace(-10/tau,10/tau,ny);
for m=1:ny
  u1=exp(j*pi*mu.*t.*t);
  u2=conj(u1).*exp(j*2*pi*fd(m)*t);
  c=conv(u2,fliplr(u1)).*dt;
  z=[z;abs(c)];
end
t=[fliplr(-t),t(2:nx)];
figure(1)
  mesh(t,fd,z),grid
  xlabel('delay [microsec]')
  ylabel('frequency [MHz]')
  zlabel('magnitude')
figure(2)
  contour(t,fd,z,5),grid
  xlabel('delay [microsec]')
  ylabel('frequency [MHz]')
figure(3)
  plot(t,z((ny+1)/2,:),'w')
  xlabel('delay [microsec]')
  ylabel('magnitude')
figure(4)
  plot(fd,z(:,nx),'w')
  xlabel('frequency [MHz]')
  ylabel('magnitude')
```

```
% Filename: program5.m
% Title: Ambiguity function of the step frequency radar by the correlation method
% Date of last revision: 26 Apr 1996
% Written by: Paulo A. Soares
% Comments: This program computes and plots several figures of the ambiguity function of the
%               step frequency radar, using the correlation method.
%******************************************************************************


%-----------------------------------------------------------------------------------------------------
%                                      Parameters initialization
%-----------------------------------------------------------------------------------------------------
clear;                              % clears all variables
tau=1;                             % tau=pulse width
T=5;                               % T=period or pulse repetition interval (PRI)
N=10;                              % N=number of pulses
df=1;                              % df=frequency step
sampfreq=40;                       % sampfreq=sampling frequency
NT=N*T;                            % NT=total period of the waveform
nsamptau=sampfreq*tau;             % nsamptau=number of samples in one pulse width
nsampt0=sampfreq*(T-tau);          % nsampt0=number of samples in the interpulse period
nsamptau=floor(nsamptau);
nsampt0=floor(nsampt0);
nsampT=nsamptau+nsampt0;           % nsampT=number of samples in one PRI


%-----------------------------------------------------------------------------------------------------
%                                      Definition of axis and resolution
%-----------------------------------------------------------------------------------------------------
P=[ones(1,nsamptau),zeros(1,nsampt0)];
t=linspace(0,NT,N*nsampT);                 % time axis definition
ny=301;                                    % number of points in the freq. axis
fd=linspace(-5/T,5/T,ny);                  % freq. axis definition
dt=t(2)-t(1);                              % dt=time interval


%-----------------------------------------------------------------------------------------------------
%                                      Computations
%-----------------------------------------------------------------------------------------------------
s=[];
m=1:1:N;
for n=1:N
 s=[s,exp(j*2*pi*(m(n)-1)*df*t(nsampT*(n-1)+1:nsampT*n)).*P];
end
z=[];
for L=1:ny
 f=fd(L);
 s1=conj(s).*exp(j*2*pi*f*t);
 s2=s;
 c=conv(s1,fliplr(s2)).*dt;
 %z=[z;(abs(c)).^2];
 z=[z;abs(c)];
end
[l,r]=size(z);
t=[fliplr(-t),t(2:N*nsampT);
```

```
%----------------------------------------------------------------------------------------------------
%                                    Plotting of the results and axis labeling
%----------------------------------------------------------------------------------------------------
figure(1)
 mesh(t,fd,z),grid
 xlabel('delay [microsec]')
 ylabel('frequency [MHz]')
figure(2)
 contour(t,fd,z,5)
 axis([-10 10 -1 1])
 xlabel('delay [microsec]')
 ylabel('frequency [MHz]')
figure(3)
 plot(t,z((ny+1)/2,:))
 axis([-30 30 0 12])
 xlabel('delay [microsec]')
 ylabel('magnitude')
figure(4)
 plot(fd',z(:,(r+1)/2),'w')
 xlabel('frequency [MHz]')
 ylabel('magnitude')
figure(5)
 contour(t,fd,z,5)
 axis([-1.5 1.5 -0.2 0.2])
 xlabel('delay [microsec]')
 ylabel('frequency [MHz]')
figure(6)
 plot(t,z((ny+1)/2,:))
 axis([-1.5 1.5 0 12])
 xlabel('delay [microsec]')
 ylabel('magnitude')
figure(7)
 plot(fd',z(:,(r+1)/2)')
 xlabel('frequency [MHz]')
 axis([-0.12 0.12 0 6])
```

```
% Filename: program6.m
% Title: Ambiguity function of the step frequency radar by the equation method
% Date of last revision: 26 Apr 1996
% Written by: Paulo A. Soares
% Comments: This program computes and plots several figures of the ambiguity function of the
%           step frequency radar, using the equation method.
%*********************************************************************************
%-------------------------------------------------------------------------------
%                              Parameters initialization
%-------------------------------------------------------------------------------
clear;                          % clears all variables
tau=1;                          % tau=pulse width
T=5;                            % T=pulse repetition interval (PRI)
N=10;                           % N=number of pulses
df=1;                           % df=frequency step
d=tau/T;                        % d=duty cycle


%-------------------------------------------------------------------------------
%                              Definition of axis and resolution
%-------------------------------------------------------------------------------
nx=101;                              % nx=number of points in the time axis
t=linspace(-N*T,N*T,nx);             % time axis definition
ny=3001;                             % ny=number of points in the freq. axis
fd=linspace(-5/T,5/T,ny);            % freq.axis definition
%-------------------------------------------------------------------------------
%                              Computations
%-------------------------------------------------------------------------------
p=floor(t/T);
r=(t/T)-p;
z=[];
for m=1:ny
x=[];
f=fd(m);
for n=1:nx
pp=p(n);
rr=r(n);
f1=f-pp*df;
f2=f-(2*pp+rr)*df;
f3=f-(pp+1)*df;
f4=f-(2*pp+rr+1)*df;
if rr>=0 & rr<d
  if f1==0
   x1=1;
  else
   x1=(sin(pi*f1*(tau-rr*T)))./(pi*f1*(tau-rr*T));
  end
  if rem(f2*T,1)==0
   x2=N-abs(pp);
  else
   x2=(sin(pi*f2*(N-abs(pp))*T))./(sin(pi*f2*T));
  end
  x=[x,(tau-rr*T).*x1*x2];
elseif rr<1 & rr>=(1-d)
  if f3==0
   x1=1;
```

```
  else
    x1=(sin(pi*f3*(tau+(rr-1)*T)))./(pi*f3*(tau+(rr-1)*T));
  end
  if rem(f4*T,1)==0
    x2=N-abs(pp+1);
  else
    x2=(sin(pi*f4*(N-abs(pp+1))*T))./(sin(pi*f4*T));
  end
  x=[x,(tau+(rr-1)*T).*x1*x2];
else
  x=[x,0];
end
end
z=[z;x];
end
z=abs(z);


%------------------------------------------------------------------------------------------------
%                        Plotting of results and axis labeling
%------------------------------------------------------------------------------------------------
figure(1)
 mesh(t,fd,z),grid
 xlabel('delay [microsec]')
 ylabel('frequency [MHz]')
figure(2)
 contour(t,fd,z,5)
 axis([-6 6 -0.2 0.2])
 xlabel('delay [microsec]')
 ylabel('frequency [MHz]')
figure(3)
 plot(t,z((ny+1)/2,:))
 xlabel('delay [microsec]')
 ylabel('magnitude')
figure(4)
 plot(fd',z(:,(nx+1)/2)')
 xlabel('frequency [MHz]')
 ylabel('magnitude')
figure(5)
 contour(t,fd,z,5')
 axis([-0.7 0.7 -0.05 0.05])
 xlabel('delay [microsec]')
 ylabel('frequency [MHz]')
figure(6)
 plot(t,z((ny+1)/2,:))
 axis([-1.5 1.5 0 12])
 xlabel('delay [microsec]')
 ylabel('magnitude')
figure(7)
 plot(fd',z(:,(nx+1)/2)')
 axis([-0.05 0.05 0 0.5])
 xlabel('frequency [MHz]')
 ylabel('magnitude')
```

LIST OF REFERENCES

1. Merill I. Skolnik, *Introduction to Radar Systems*, Second Edition, McGraw-Hill, Inc., 1980.

2. Donald R. Wehner, *High Resolution Radar*, Second Edition, Artech House Inc., 1995.

3. Byron Edde, *Radar. Principles, Technology, Applications*, Prentice-Hall, Inc., 1993.

4. George W. Stimson, *Introduction to Airborne Radar*, Hughes Aircraft Company, 1983.

5. Nicholas C. Currie, *Radar Reflectivity Measurement: Techniques & Applications*, Artech House, Inc., 1989.

6. James A. Scheer, and James L. Kurtz, *Coherent Radar Performance Estimation*, Artech House Inc., 1993.

7. Nadav Levanon, *Radar Principles*, Wiley & Sons, Inc., 1988.

INITIAL DISTRIBUTION LIST

1. Defense Technical Information Center 2
   8725 John J. Kingman Rd., STE 0944
   Ft. Belvoir, VA 22060-6218

2. Dudley Knox Library 2
   Naval Postgraduate School
   411 Dyer Rd.
   Monterey, CA 93943-5101

3. Chairman, Code PH 1
   Department of Physics
   Naval Postgraduate School
   Monterey, CA 93943-5117

4. Professor Gurnam S. Gill, Code EC/Gl 5
   Department of Electrical and Computer Engineering
   Naval Postgraduate School
   Monterey, CA 93943-5121

5. Professor Suntharalingam Gnanalingam, Code PH/Gm 1
   Department of Physics
   Naval Postgraduate School
   Monterey, CA 93943-5117

6. Direcção do Serviço de Formação 1
   Administração Central de Marinha
   Rua do Arsenal
   1100 Lisboa
   Portugal

7. LT Paulo A. Soares 2
   Rua Ramiro Ferrão 18, 8° Frente
   2800 Almada
   Portugal